MECH 393: Machine Element Design

Final Project Report: Plane Gearbox

Thomas St-Cyr – 261113945

William Van Hove – 261119889

Yingtong Luo – 261009206

Elaine Yang – 261022515

Prof. Larry Lessard

TA: Sebastian MacDonald

December 4th, 2024

1. Abstract

This report details the design and analysis of a double-reduction gearbox for Solar Impulse, a solar powered electric aircraft aimed at promoting sustainability in aviation. As a critical component of the aircraft's propulsion system, the gearbox was designed to efficiently transmit power while adhering to aerospace regulations and the companies' standards for weight, size, performance, reliability, and safety. The primary objective was to create a compact, lightweight, and energy-efficient gearbox capable of reducing an input rotational speed of 5500 RPM to a desired output of 835 RPM, achieving a minimum gear ratio of 6.587, with a safety factor of at least 1.5 for all components.

The gearbox design considered gears, shafts, keys, and bearings for the scope of this project. Gears were designed first, then shafts, and lastly keys and bearings were done simultaneously. The gears were designed following AGMA standards, and optimized using Python to minimize weight and size, without compromising strength and durability. The optimal gear teeth combination is the following: 21 (gear 1), 59 (gears 2 and 2'), 19 (gears 3 and 3'), and 45 (gear 4). Titanium and AISI steel are the two materials chosen for gears due to their weight ratios. Then, bending and surface safety factors were verified to exceed 1.6.

Shafts were then designed by first choosing suitable AISI steel, and then a stress and fatigue analysis was conducted to determine the shafts diameter and related geometric dimensions, using a safety factor of at least 1.75. Major shaft diameters were rounded to standard sizes and are the following: 0.6875 inches for input shaft 1, 1.0 and 1.1875 inches for shafts 2 and 3, and 1.375 inches for output shaft 4. Keys were then designed from suitable steel with standard US sizes. Key lengths were adjusted so that each keys had a safety factor of at least 1.5 either in shear or bearing failure to ensure that they break first in the event of an overload. Bearings were selected from the SKF catalog to meet the gearbox's lifespan requirements.

The final gearbox has a mass of $15.839\ kg$, and measures $25 \times 35.814 \times 15.494\ cm$, meeting Solar Impulse's design specifications. The proposed solution then supports the broader mission of reducing greenhouse gas emissions in aviation and advancing the feasibility of solar-powered electric aircrafts. This report will provide an in-depth insight into the design methodology, component analysis, optimization, project limitations, and final solution.

Table of Contents

2. Introduction

2.1 Problem Statement

With increasing global temperatures, rising sea levels, and increased frequency of natural disasters, evidence for climate change is accumulating. The aviation sector, a major contributor to climate change due to reliance on petroleum-based jet fuels and high greenhouse gas (GHG) emissions, must adopt serious measures to reduce its carbon footprint. Because of the desire for a greener aviation future, many researchers and companies are now investigating sustainable energy sources such as solar and electric energy.

Solar Impulse, a Swiss project focused on solar-powered aviation, aims to design an aircraft capable of circumnavigating the globe using only solar energy. The project engineers now require a new gearbox design to complete the electric propulsion system of their aircraft and have contacted our team to complete this task. Since technologies using solar energy have lower power density than conventional combustion engines, weight is a critical factor as well as energy efficiency to ensure the long-range performance required. While budget is not a concern, Solar Impulse emphasizes the importance of minimizing weight, optimizing energy efficiency, ensuring endurance, and meeting certification standards.

In subsequent communications with Solar Impulse, the chief engineer proposed changing the gearbox design from a single to a double reduction gearbox. He provided the design requirements for the new gearbox, along with key specifications about the propeller and flight performance, which are detailed in *Appendix A*.

2.2 Approach

Following the chief engineer's directives, the double reduction gearbox is to be compact, lightweight, energy-efficient, and certification-compliant. All components – gears, shafts, bearings, and keyways – will be designed according to the American Gear Manufacturers Association (AGMA) standards for spur gears.

To maximize energy efficiency and ensure proper load distribution, the gearbox will consist of six gears of four different sizes, and four shafts: two identical due to symmetry, and separate input and output shaft. *Figure 1* below illustrates the proposed design. The double reduction gearbox operates by reducing the rotational input speed through two gear ratios in a two-stage reverted compound gear train, utilizing three shafts. The bottom shaft serves to reduce the load transmitted by each gear.

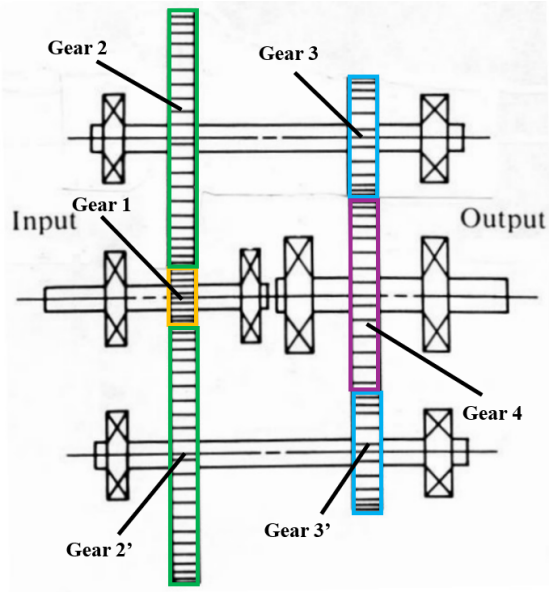

Figure 1: Representation of the Double Reduction Gearbox

For the remainder of this report, the shafts will be labeled as follows: the input shaft as shaft 1, the top and bottom shafts as shaft 2 and shaft 3, and the output shaft as shaft 4. The gears will be labeled as: gear 1 (G1) for the first pinion on the input shaft, gear 2 (G2) for the first gear on shaft 2, gear 3 (G3) for

the pinion on the right of shaft 2, and gear 4 (G4) for the last gear on the output shaft. Additionally, gear 2' (G2') refers to the gear on the left of shaft 3, and gear 3' (G3') refers to the pinion on the right of shaft 3.

For simplicity, the gearbox was designed assuming only three shafts, ignoring shaft 3's specific design but accounting for its effects on the gearbox, since shafts 2 and 3 are symmetrical and designed to be identical.

To ensure the proposed gearbox meets Solar Impulse's durability criteria, the loads considered correspond to the aircraft operating at maximum capacity. Specifically, these loads are based on the plane being in take-off configuration 100% of the time, with an input spit of 5500 RPM and a desired output speed of 835 RPM. Though, for the number of cycles, the true speed values for each flight stage were used.

Given the complexity of the task at hand, the design process was organized based on the interdependencies of the components. For instance, gear 1's bore diameter is determined by the input shaft's diameter. The design proceeded in the following sequence: first, the main parameters for the gears were established, followed by the shafts and keyways, and finally, the keys and bearings were designed simultaneously. Of course, certain design parameters determined later during the process affected certain decisions made earlier on. The required modifications were then made accordingly to have a complete and cohesive design.

3. Theoretical Development

The objective of this project is to a double reduction gear box for a small solar-powered airplane, focusing on optimizing weight and size.

This section will discuss the optimization methods, key equations, relevant standards, and the rationale behind the final design decisions. As previously mentioned, due to interdependencies among various mechanical components, the design process follows this specific order: gears, shafts, keys, and bearings, although keys and bearings can be done simultaneously.

The gearbox design is governed by several key constraints reflecting the operational needs of the solar-powered aircraft. A primary consideration is the safety factor, set at 1.5 as per aerospace industry standards [1]. This conservative value ensures that the gearbox can withstand unpredictable loads such as turbulence and accounts for the cyclic loading that results in material fatigue. To increase reliability and guarantee structural integrity, it is essential that the keys fail first, preventing damage to more critical and expensive components such as gears or shafts and therefore minimizing catastrophic failures and associated repair costs. To ensure a predictable failure order of the mechanical components, the safety factor for gears is set to 1.6, slightly higher than that of the key, while the shafts are assigned a safety factor of 1.75 which ensures that they fail last. *Table 1* below summarizes the desired safety factor for various components of the gearbox

Table 1: Desired Safety Factor for Different Gearbox Components and Acceptable Ranges

Component	Desired Safety Factor	Acceptable Range
Keys	1.5	$1.5 \leq N_{key} < 1.6$
Gears	1.6	$1.6 \leq N_{gear} < 1.75$
Shafts	1.75	$N_{shaft} > 1.75$

It should be noted that the above desired safety factor and acceptable range serve only as guidelines for analysis. For example, if all gears fall within the acceptable range presented except one with a higher safety factor than the shafts, the design remains acceptable, as the weakest gear will fail before any shaft. In other words, not all gears have to be weaker than the shafts, only one.

3.1 Gear Design

From a performance standpoint, the gearbox must guarantee that the maximum rotational output speed does not exceed 835 RPM under any operating conditions. Also, it is constrained by a geometric envelope with a maximum span of 30 $cm \times 45\ cm \times 45\ cm$ box accounting for the limited space within the aircraft.

The design must also meet a 2000-hour lifespan requirement which hints at the necessity to select durable materials and a fatigue-resistant design. In addition, the gearbox must operate within a temperature range of -40 ℃ to 40℃ to be suitable for harsh flight environments.

The gearbox must also accommodate for varying rotational speeds and power demands during various flight stages, requiring a flexible and robust design. Minimizing weight is also critical, as reduced gearbox mass enhances efficiency and thereby aircraft performance.

3.1.1 Design Background and Constraints

The gearbox is crucial for transmitting torque and reducing angular velocity between the input and output shafts while meeting aerospace constraints on weight, safety, and robustness. In this double reduction gearbox, this is done sequentially through two gear sets. The selected design contains a total of six spur gears to achieve the required speed reduction.

The gear train configuration, shown in *Figure 1* above, includes input gear 1 (pinion) meshing with intermediate gears 2 and 2' which are mounted coaxially with gears 3 and 3'. These intermediary gears mesh with the output gear 4, thus completing the reduction process. Through this setup, the angular velocity from the motor is reduced to the desired velocity for the propeller. As mentioned, all gears are designed according to the AGMA (American Gear Manufacturers Association) standards to ensure reliability and performance.

3.1.2 Gear Ratio Optimization & Algorithm-Based Design

To achieve the required performance and minimize weight, the two-stage speed reduction gearbox must optimally distribute the total gear ratio of 6.587 between the two gear sets. This ratio is derived from the maximum input angular speed during take-off: 5500 RPM, and the desired output speed: 835 RPM. The total gear ratio is determined by calculating the angular velocity ratio m_v and the torque ratio m_A, with the gear ratio chosen as whichever value is greater than 1. The value of 6.587 is obtained using 5500 RPM as the input velocity and 835 RPM as the output velocity.

In this project, the double reduction gearbox's total gear ratio is the product of the individual gear train ratios. As per the design requirements, the output velocity must not exceed 835 RPM; thus, the total gear ratio computed should be as close as possible to this value without being smaller to optimize output.

To meet design constraints and minimize weight, a Python-based numerical optimization approach was used to efficiently determine the optimal teeth number combination. This method analyzes two variable functions within a defined range, offering significant advantage by avoiding manual calculations. The algorithm used incorporates constraints and iteration criteria to ensure practical results that meet design standards and requirements.

I. Minimum Total Gear Ratio

The primary constraint is that the total gear ratio of the two-stage reduction gearbox must exceed 6.587. To account for errors in the optimization process, the threshold is set to 6.6, with only solutions meeting or exceeding this value considered valid. See *Appendix D.1* for gear ratio calculations.

II. Integer Gear Teeth Number

All gear teeth numbers must be integers, as fractional teeth are impossible to manufacture. If fractional teeth numbers are obtained, the value will be round up to the nearest integer to satisfy this criterion.

III. Diametral Pitch Limitation

The diametral pitch p_d of all gears must be coarse with p_d less than 20. In the aerospace industry, gears with larger teeth are generally preferred due to their easier manufacturability, greater contact area, and superior wear resistance [2]. This constraint ensures that the gears are suitable for the high-performance requirements of aerospace applications.

IV. Minimum Number of Teeth

The gears used in this design are selected to have AGMA full-depth teeth standard, with a pressure angle of 20 degrees. To avoid undercutting or interference, the minimum number of teeth is calculated to be 18 using the equation below, where $\emptyset$ denotes the pressure angle of the gear.

$$N_{min} = \frac{2}{sin^2\emptyset} \quad (1)$$

This criterion ensures smooth operation of the gearbox.

V. Individual Gear Ratio Limitation

General guidelines limit individual gear ratios to a maximum of 1:10 to avoid excessive torque loads. Thus, the algorithm will iterate only for ratios below this threshold.

VI. Matching diametral Pitch for Mating Gears

To ensure proper meshing, the diametral pitch of any two mating gears must be identical.

VII. Shaft Alignment Criterion

All three shafts involved in this gearbox design should be parallel to ensure smooth power and torque transmission. Also, due to symmetry, the input and output shaft must be concentric. Hence, the diameters of the gears in both sets should be carefully designed so that they satisfy the following geometric relation:

$$R_1 + R_2 = R_3 + R_4$$

If this expression is written in terms of p_d and teeth number, the formula can be re-expressed as:

$$\frac{N_1}{p_{d_1}} + \frac{N_2}{p_{d_1}} = \frac{N_3}{p_{d_2}} + \frac{N_4}{p_{d_2}}$$

In the subsequent sections, the implementation of the numerical method, including its structure and results, will be discussed in detail.

The optimization algorithm begins by setting a total gear ratio target of 6.6. Once the gear ratio for set 1 is selected, the ratio for set 2 is automatically determined, as the product of the individual gear ratios must equal the total gear ratio of the compound train. This relationship is expressed mathematically as:

$$r_{total} = r_1 \times r_2$$

To account for various possibilities in gear teeth combination, the range of the first gear set's ratio is set to vary from 1.8 to 3.8, with an iteration step size of 0.1.

Next, three validation functions are defined based on the criteria outlined. First, each gear's minimum teeth number must be at least 18. Second, concentricity is verified. Lastly, the y-span for both gear sets is calculated, with the larger value representing the widest part of the gear train. Any combination with a y-span exceeding 45 cm is automatically rejected by the algorithm.

A system of equations can be developed based on the compound gear configuration and can be used to find all gear teeth numbers if proper initial "guess" is given. The relationship between gears is shown below:

$$\frac{N_2}{N_1} = r_1 \qquad \frac{N_3}{N_4} = r_2$$

$$\frac{N_1}{P_{d_1}} + \frac{N_2}{P_{d_1}} = \frac{N_3}{P_{d_2}} + \frac{N_4}{P_{d_2}}$$

In this algorithm, we select the gear 2 teeth number as the initial guess. The number of teeth for gear 2 varies from 18 (minimal allowed value) to 120. Subsequently, the values of N_1, N_3, and N_4 can be expressed in terms of known variables N_2, P_{d_1}, P_{d_2}, r_1, and r_2. Thus, the system has three equations and three unknowns and can be solved numerically.

The solution from every iteration will be set as an input to the three validation functions and the valid solutions will be stored in a list for further data analysis.

Finally, all gears are approximated as cylinders with height equal to the face width and the base diameter equal to the pitch diameter. This allows for easy computation of gear volume and mass, with the lightest solution among the valid combinations selected as the final choice. A sample script containing the iterative criteria is provided in *Appendix B*.

3.1.3 Design of Gear Geometry

The selection of diametral pitch p_d and face width F is crucial for optimizing the balance between strength, weight, and safety in the gearbox design as they directly influence stress distribution, load-carrying capacity, and gear weight. This section outlines the methodology for determining appropriate p_d and face width values to meet all operational and safety requirements.

Determining p_d was an iterative process aimed at optimizing gear strength while avoiding overdesign. Initially, the possibility of using the same p_d for both gear sets was considered, but it was deemed unsuitable due to the significant torque transmission differences between the input and output gear sets.

Based on the pre-determined gear ratio and maximum input power, the torques on the gears are calculated. At maximum power, the input gear experiences a torque of $57.3\ lb \cdot ft$, while the output gear endures a torque of $381.25\ lb \cdot ft$ which is seven times greater. See *Appendix D.6* for torque sample calculations. Since the teeth number and face width of the gears in both sets are similar, using the same p_d value for both sets would lead to overdesign, particularly for gear set 1. Specifically, to ensure all gears meet the required safety factor, some gears would need to be significantly oversized, increasing unnecessarily the weight of the gearbox.

A more effective approach involved assigning distinct diametral pitch values to the two gear sets, allowing for independent optimization based on the torque each set transmits. Additionally, since p_d directly affects the face width according to the relationship $F = \frac{x}{p_d}$, where x ranges from 8 to 16 [2]. Considering the higher torque and stress experienced by the output gear set, its p_d value was set to 10 after iteration resulting in a smaller face width. This decision leads to increased contact area, reducing the contact stress and improving the safety factor for the output gears. As for the first gear set, the p_d value was set to 8 resulting in a greater face width. Both values conform with the standard options available in US customary units, ensuring manufacturability and consistency with industry practices.

The face width of a gear significantly influences its load-carrying capacity and overall weight. A larger face width provides a greater contact area between gears, reducing stress and increasing the safety factor. However, increasing the face width also adds weight, which is a critical consideration for the lightweight design of this solar-powered aircraft.

To determine the optimal face width, we analyzed the trade-off between strength and weight. Using the relationship $F = \frac{x}{P_d}$, we systematically varied x value to evaluate its impact on the safety factor and weight. For each iteration, the face width was tested against the required safety factor of 1.6, considering the operational torque and loading conditions. After extensive evaluation, the optimal solution was achieved when $x = 13$. This value provided sufficient load-carrying capacity while minimizing the additional weight. The face width for each gear set was then calculated based on the corresponding p_d, ensuring that the design met all strength and safety requirements without unnecessary overdesign.

3.1.4 Gear Life Cycle Analysis

The life cycle analysis of a gearbox is crucial in assessing its reliability under varying operational conditions. The target lifespan is 2000 hours, approximately equivalent to 667 flight missions by simplifying the flight time to three hours. This estimate involves reducing the durations of the low-gradient flight and steep-gradient climb phases from 15 minutes to 10 minutes, thus facilitating calculation while maintaining conservativeness in the analysis. Each flight consists of five distinct phases with significant variations in input power and rotational speeds as shown in *Appendix A*.

Over the gearbox's 2000-hour lifespan, the total time spent in each flight phase can be calculated. For 667 flights, the takeoff, slow climb, and steep climb phases each account for approximately 6670 minutes while the descent phase totals 20000 minutes. The cruise phase, which is the longest, contributes 80000 minutes. This detailed breakdown of the time distribution across flight stages is essential for assessing the gearbox's fatigue behavior. These durations are summarized in *Table D.8.1*.

The number of load cycles experienced by each gear varies depending on its position in the gear train and the speed ratios. Gears that mesh with two others, such as the input and output gear experience double the load cycles of intermediate gears. Using the speed ratios of 21:59:19:45, the total cycle counts over the

gearbox's life are calculated. Gear 1 experiences approximately 261,063,800 cycles, gears 2 and 3 each undergo 111,984,778 cycles, and gear 4 completes 94,564,924 cycles.

The calculation results are tabulated in *Table 2* below for future reference. These values incorporate conservative rounding practices, ensuring that the estimated cycle counts are greater than the actual cycle numbers. A sample calculation for the time distribution breakdown and the number of cycles is provided in *Appendix D.8*.

Table 2: Number of Loading Cycles on Different Gears

Gear number	Gear 1	Gear 2 and 2'	Gear 3 and 3'	Gear 4
Gear classification	Pinion	Gears	Pinions	Gear
Number of cycles	261,063,800	111,984,778	111,984,778	94,564,924

3.1.5 Load and Stress Analysis

First, the torques in each gear must be computed using the following equation:

$$P = T\omega \tag{2}$$

where P is the engine power assumed to be constant considering steady maximum operational regime.

During the operation of the gear, torque will be transmitted from the pinion to the gear. At the pitch point, ignoring the friction generated by the gear contact, only force W will be transmitted from the pinion teeth to the gear teeth along the pressure angle. This force W consists of two parts: radial and tangential components. The FBD diagrams of the gear set are shown in *Figure 2* below. When exploring the bending stress and surface stress between gears in this project, only the tangential component needs to be considered. The tangential load W_t can be calculated using the following:

$$W_t = T_p / \frac{d_p}{2} \tag{3}$$

where T_p is the torque on the pinion shaft and d_p is the pitch diameter.

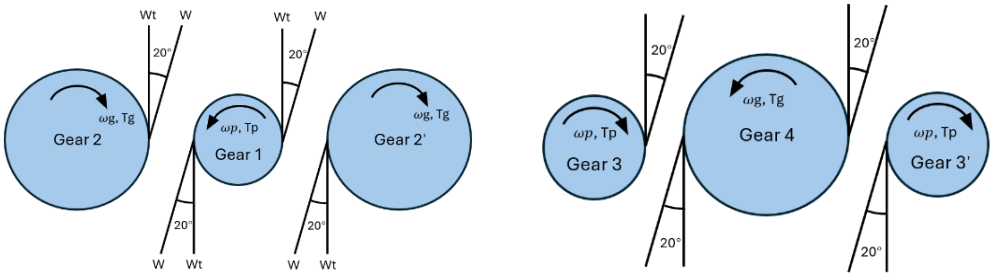

Figure 2: FBD Diagrams of Group 1 Gears (Left) and Group 2 Gears (Right)

I. Bending Stress

After the determination of transmitted load acting on each gearset, the bending stress σ_b acting on each pinion and gear can be calculated by the bending stress equation [2],

$$\sigma_b = \frac{W_t p_d}{FJ} \frac{K_a K_m}{K_v} K_S K_B K_I \tag{4}$$

where F is the face width; J is the geometry factor; K factors are modifiers to account for various conditions.

To use the equation above, few assumptions are made about the tooth and gear-mesh geometry [2]: 1) There is no interference between the tips and root fillets of the mating teeth and no undercutting of teeth above the theoretical start of the active profile. 2) No teeth are pointed. 3) There's nonzero backlash. 4) The root fillets are standard, smooth, and produced by a generating process. 5) The friction forces are neglected. The reasoning and assumptions made in selection of correction factors are introduced below.

i. *J* Bending Strength Geometry Factor

Since a full depth involute profile AGMA spur gearset was required and the pressure angle is 20°, *Table C.1* in *Appendix C* should be chosen to determine the value of J. The reason for using HPSTC Loading is because a high-precision gearbox is needed for the aircraft [2].

ii. K_v Dynamic Factor

The dynamic factor is used to account for internally generated vibration loads, also known as transmission error, from the tooth contact impacts induced by nonconjugate meshing of the gear teeth. In the absence of test data defining the level of transmission error expected in the gear design, K_v can be read from *Figure C.2* in *Appendix C*, in which Q_v is the b index, V_t is the pitch-line velocity. According to *Figure C.3* in *Appendix C*, for aircraft engine drive, $Q_v = 11$ is a reasonable value.

iii. K_m Load Distribution Factor

The load distribution factor depends on the value of face width F. According to *Figure C.4* in *Appendix C*, the value of K_m can be determined.

iv. K_a Application Factor

The transmitted load W_t is assumed to be uniform during the motor operation. Therefore, according to *Figure C.5* in *Appendix C*, K_a=1.

v. K_s Size Factor

Since there is no geometry situation such as large teeth needed to consider, K_s is set to 1.

vi. K_B Rim Thickness Factor

The rim thickness factor depends on the rim-tooth ratio, $m_B = t_R/h_t$, where t_R is the rim thickness from the tooth root diameter to the rim's inside diameter. h_t is the whole depth of the tooth. In this case, the rim thickness is much larger than the whole depth of the tooth. Therefore, according to the empirical formula, K_B=1, and for conservative purpose, K_B can be set between 1.25~1.5.

vii. K_I Idler Factor

Since no idler gears are involved in both gearsets, K_I=1.

To obtain the safety factors for bending, the bending-fatigue strengths for gear materials should be determined first by equation:

$$S_{fb} = \frac{K_L}{K_T K_R} S_{fb'} \tag{5}$$

where S_{fb} is the corrected strength; $S_{fb'}$ is the published AGMA bending-fatigue strength, which is approximated by equation $S_{fb'} = 102HB + 16400$ [2], where HB is the Brinell Hardness of material. K factors are modifiers to account for various conditions, which will be discussed below.

i. K_L Life Factor

The life factor is calculated using the equation for the lower portion of the shaded area in *Figure C.6* in *Appendix C*, since this design is used for critical service applications [2]. Substituting in the life cycle of pinion and gear separately can obtain the value of K_L.

ii. K_T Temperature Factor

The temperature factor is calculated using the following equation [2]:

$$K_T = \frac{460 + T_F}{620} \tag{6}$$

where T_F is the motor operating temperature range in Fahrenheit. According to the design requirements, the operation temperature range is 250 °F. Therefore, $K_T = 0.9097$ for all cases.

iii. K_R Reliability Factor

Since the gearbox is designed for an aircraft motor, it is reasonable to percent of reliability to 99%. Therefore, according to *Figure C.7* in *Appendix C*, K_R=1.

The safety factor for bending, N_b, then is calculated by the ratio of S_{fb} to σ_b.

II. Surface Stress

Since mating gear teeth have a combination of rolling and sliding at their interface, the potential surface failure on the teeth must be considered. The surface stress σ_c at the mating point is calculated by formula [2]:

$$\sigma_c = C_p\sqrt{\frac{W_t}{FId}\frac{C_aC_m}{C_v}C_sC_f} \tag{7}$$

where W_t is the tangential force on the tooth, d the pitch diameter of the pinion, F the face width, and I is a dimensionless surface geometry factor for pitting resistance. C_p is the elastic coefficient that accounts for the difference in the gear and pinion material constants. The C factors except C_f, are equal to the K factors with the same subscript as defined for the bending stress equation and new correction factors introduced will be discussed below.

i. I Surface Geometry Factor

This factor considers the radii of curvature of the gear teeth and the pressure angle. The equation for I is defined by AGMA [2]:

$$I = \frac{cos\varphi}{\left(\frac{1}{\rho_1}+\frac{1}{\rho_2}\right)d_p} \tag{8}$$

Where ρ_1 and ρ_2 are the radii of curvature of the pinion and the gear teeth respectively, d_p is the pitch diameter of the pinion, and φ is the pressure angle.

ii. C_p Elastic coefficient

The elastic coefficient accounts for differences in tooth materials and is found from equation below:

$$C_p = \sqrt{\frac{1}{\pi\left[\left(\frac{1-v_p^2}{E_p}\right)+\left(\frac{1-v_g^2}{E_g}\right)\right]}} \tag{9}$$

where, E_p and E_g are the modulus of elasticity for pinion and gear respectively, and v_p and v_g are their respective Poisson's ratios.

iii. C_F Surface Finish Factor

This factor is used to account for unusually rough surface finishes on gear teeth and can be set to 1 for gears made by conventional methods, which is applicable to this gearbox design.

Before calculating the safety factors for surface stress, the surface-fatigue strengths for pinion and gear should be determined by equation:

$$S_{fc} = \frac{C_LC_H}{C_TC_R}S_{fc'} \tag{10}$$

where S'_{fc} is the published AGMA surface-fatigue strength and is approximated by $S'_{fc} = 349HB + 34300$ [2]. S_{fc} is the corrected strength and C factors being the modifiers to account for various conditions. Factors C_T and C_R are the same as K_T and K_R mentioned in bending-fatigue strength, and the new C factors will be explained below:

i. C_L Surface Life Factor

The life factor is calculated using the equation for the lower portion of the shaded area *in Figure C.9* in *Appendix C*, since this design is used for critical service applications. Substituting in the life cycle of pinion and gear separately can obtain the value of C_L.

ii. C_H Hardness Ratio Factor

This factor is a function of the gear ratio and the relative hardness of pinion and gear, and acts to increase the apparent strength of the gear. In the absence of the RMS surface roughness of pinion teeth, both pinion and gear are assumed through-hardened. The formula of C_H for through-hardened pinions and gears is [2]:

$$C_H = 1 + A(m_G - 1) \tag{11}$$

where m_G is the gear ratio. Then, the safety factors of surface stress in the gearset are obtained by the ratio of S_{fc} to σ_c.

3.1.6 Material Selection

The gear's material selection focused on two key requirements: the ability to withstand operational loads and stress with a minimum safety factor of 1.5 and minimizing weight to meet performance and efficiency goals. Strength, ductility, hardness and density were the primary criteria for evaluating material combinations for the pinion and gear. Various properties of the candidate materials are provided in *Appendix D.9*.

Though the criteria mentioned are necessary, their importance varies based on the gear and its location in the gearbox. Indeed, in a gear set, the pinion will experience much higher stress than the gear. As a result, the pinion might require stronger and harder material than the gear, Also, the torque in the gearbox is not constant, varying from one shaft to another, which might result in a gear set requiring stronger gear and pinion. All of this was considered in the material selection process leading to the final material combination presented in the *Results* section.

3.2 Shaft and Keyway Design

3.2.1 Design Background and Constraints

Shafts were the next step in the design process, along with keyways that are designed simultaneously. The overall configuration of the gearbox with each shaft is shown in *Figure 1* above. Four shafts had to be designed for this gearbox. However, shafts 2 and 3, as mentioned previously, are identical meaning that the design for one of these shafts can be used for the other as well. Its effects on the gearbox itself will not be ignored, but essentially 3 shafts must be designed. Since we know the input power and input rotational speed, it is possible to determine the torque in the input shaft as well as the torque and angular speed of the other shafts using gear ratios. The procedure is shown in *Appendix D.6*.

The design of the shafts in this mechanical assembly was less constrained than other components, with the primary limitation being weight. Indeed, although the weight must be kept as low as possible, the only physical constraint of the gearbox was its size, which is itself tied to the weight. While the gears are mostly limited in width and height, the shafts are constrained in length with a total gearbox length of maximum 30 cm to meet Solar Impulse's requirements. More precisely, the combined length of shafts 1 and 4 is set to be under 25 cm, excluding shaft extrusions connecting the motor or the propeller. The remaining 5 centimeters account for spacing between input and output shafts to prevent contact under vibration. As for shafts 2 and 3, they were constrained to 30 cm in length each. Additionally, shaft design was influenced by gear alignment, as proper meshing and load distribution required gears to be placed side by side without offset, e.g., gear 2 on shaft 2 must align with gear 1 on shaft 1.

The length of a specific shaft is influenced by many geometries and factors to consider. First, a shaft length must accommodate for the following:

I. <u>Face Width</u>

The shaft must have enough space for the sum of the face widths of all the gears mounted on it.

II. <u>Extra Distance on Each Side of The Face Width</u>

Though not required in this project, it is good engineering practice to leave extra space on each side of a gear to facilitate alignment, assembly and disassembly. Also, it provides extra space if hubs were necessary to fix the gear in place along the shaft.

III. <u>Distance Between Bearing and Shoulder Fillets</u>

Later in the report, the importance of shoulders along the shaft will be discussed. Hence, since all the shafts designed will contain shoulders, it is important to leave a bit of space between the shoulder and the bearing location to avoid interference, friction, and associated consequences.

IV. <u>Protrusion From Bearing</u>

Since the Solar Impulse airplane will be subjected to a vast range of temperatures, thermal expansion/contraction cannot be neglected. For this reason, the shafts were designed to slightly protrude from the bearings. This will prevent the shafts from contracting to a point where they do not cover the full span of the bearings.

Two primary approaches could be used for shaft design: (1) selecting a safety factor and diameter, then choosing a material that fits these parameters, or (2) selecting a material and safety factor, then determining the corresponding diameters through iteration. The second approach was used for shafts 1, 2, and 3, with a modified version for shaft 4 due to the axial force. Indeed, this force prevents the use of the standard diameter equation that will be presented later. Hence, a diameter and material were selected for shaft 4, and the resulting safety factor was calculated and verified to ensure it is within the required range.

3.2.2 Material Selection

The material for the shafts was selected early in the design process due to the chosen methodology explained above. While materials such as cast iron, nodular iron, or bronze could be used, steel was deemed the logical choice due to its high elastic modulus [2]. Assuming the gearbox is adequately sealed and free from water intrusion, corrosion-resistant materials like stainless steel or bronze were not necessary. The material requirements included high yield and ultimate tensile strength to have a resulting high endurance limit, lightweight, a good hardness, and a good toughness. Given the variability of proposed data across online sources, a material from the textbook was chosen. After comparison, Cold Rolled AISI 1045 steel was selected for its favorable strength-to-weight ratio, enhanced strength due to its carbon composition, and superior hardness and toughness. Key properties for this material are summarized in *Table 3* below [3].

Table 3: Key Mechanical Properties of Cold Rolled AISI 1045

Yield Strength		Ultimate Strength		Endurance Limit		Density
$[MPa]$	$[psi]$	$[MPa]$	$[psi]$	$[MPa]$	$[psi]$	$[g/cm^3]$
530.9	77000	627.59	91000	313.79	45500	7.85

Titanium was considered a strong candidate for the shafts due to its higher yield and ultimate tensile strength compared to steel. However, conflicting information online and lack of key material properties in the textbook such as the usual endurance limit for this material, led to the selection of steel instead.

3.2.3 Stress Concentrators

Stress concentrators are areas on a shaft where stress increases due to change in geometry, such as keyways, shoulders, grooves, or holes, making these regions more prone to failure. For the gearbox design, shoulders were strategically incorporated to axially locate components like gears and bearings, facilitate smooth diameter transitions to distribute load more efficiently along the shafts, and reduce shaft weight. Indeed, diameter reductions were applied at the extremities of the shafts where bending moments are minimal, ensuring safe operation. Additionally, keyways were included in the design to prevent relative rotational motion between gears and shafts. *Figure 3* below presents an initial representation of the four shafts designs.

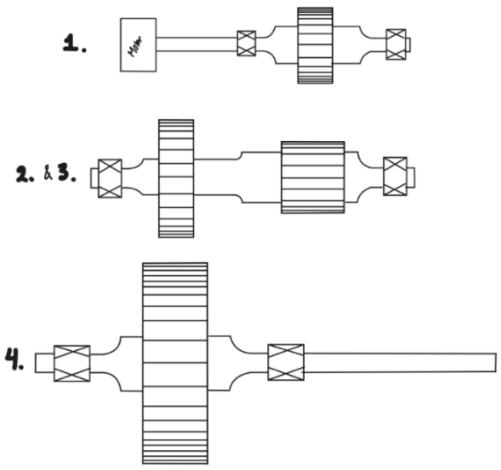

Figure 3: Approximate Shape of Input Shaft (Top), Shaft 2 & 3 (Middle), and Output Shaft (Bottom)

The stress concentrators in the gearbox shaft design are limited to keyways beneath each gear, and shoulder fillets, both serving as critical points for stress analysis. If the location along the shaft where maximum bending stress occurs is near a stress concentrator, the stress concentrator is prioritized for analysis, at its experiences higher stress.

I. Input Shaft 1

Three critical locations were identified for the first shaft: the left shoulder fillet, the keyway under gear 1, and right shoulder fillet. Due to symmetry in the shaft and load, only one shoulder fillet can be analyzed. Furthermore, the maximum bending moment occurs in the middle of the shaft where the keyway is located.

II. Shafts 2 and 3

Five to six critical points are present: the left shoulder fillet, the keyway under gear 2, the middle shoulder fillet, the keyway under gear 3, and right shoulder fillet. Asymmetry in the shafts and loads necessitates analysis of each critical location, with the maximum bending stress point analyzed if located away from these concentrators.

III. Output Shaft 4

Four critical locations are identified: the left shoulder fillet, the keyway under gear 4, the right shoulder fillet, and the point of maximum bending stress caused by the propeller load. The strong bending moment from the offset propeller load requires locating and analyzing this maximum stress point. For simplicity and due to symmetry in shoulder fillet geometry, only the worst case one is analyzed.

3.2.4 FBDs and Shear & Bending Moment Analysis

With the material and geometry of the shafts defined, shear and bending analyses were conducted. Two free body diagrams (FBDs) were created for each shaft: one illustrating the side view, showing the geometry, support reactions, gear tooth forces, and axial loads (shafts 4), and another representing the cross-section, displaying torque orientations.

This analysis was iterative and time-intensive, involving numerous FBDs with varying dimensions to minimize shaft length while achieving an optimal design. The final dimensions presented in the *Results* section are the outcome of this lengthy iterative process, and due to time constraints might not be the most optimal solution.

Using pre-calculated tangential gear forces W_t, reaction forces at the bearings were determined via static analysis, applying Newton's laws with equilibrium conditions ($\sum F_z = 0$ and $\sum M = 0$). Since gears 1 and 4 are meshing with two other gears opposed to one another, opposing gear meshing forces W_t canceled out, leaving bending moments only from the gear's weight on shaft 1 and from the combined weights of the gear and the propeller on shaft 4.

Shear and bending moment diagrams were then constructed, with moments computed at critical locations such as stress concentrators (keyways and shoulders) for further analysis. For the output shaft, bearing 6 was also analyzed as a critical point due to the propeller's weight. These diagrams and their respective important values will be discussed in detail in the *Results* section.

3.2.5 Determination of Diameters with Set Safety Factor (Shaft 1 and Shaft 2 & 3)

The diameters for shafts 1, 2, and 3, including eth smaller diameters for bearings and major diameters for gears, were determined using consistent methodology. While aerospace applications typically use a safety factor of 1.5, a more conservative safety factor of 1.75 was applied to shafts to ensure that they fail last, as previously discussed.

I. Stress Concentration Factors

Stress concentration factors are determined from values provided in the tables in the textbook which are given in the *Appendix* as *Figures C.10 to C.12* and with the following equation:

$$K_t \cong A\left(\frac{r}{d}\right)^b \tag{12}$$

Where A and b are values found in tables depending on the ratio of big diameter over small diameter D/d and the type of loading applied to the shaft, and K_t is the stress concentration factor for bending stress ($K_{t,b}$), axial stress ($K_{t,a}$), and torsional shear stress (K_{ts}).

Fatigue stress concentration factors can now be found using the notch sensitivity q as follows:

$$K_f = 1 + q(K_t - 1) \tag{13}$$

Where K_f is the fatigue stress concentration factor for bending stress ($K_{f,b}$), axial stress ($K_{f,a}$), and torsional shear stress. The notch sensitivity is computed using the following formula:

$$q = \frac{1}{1+\frac{\sqrt{a}}{\sqrt{r}}} \tag{14}$$

Where a is Neuber's constant, found using *Figure C.13* in *Appendix C*, and r is the radius of the stress concentration factor. Note that for torsional loads, Neuber's constant is found in the tables using a value of $S'_{UT} = S_{UT} + 20\ kpsi$.

For keyways, the stress concentration factor depends on whether there is a key in place transmitting torque or not, and the value is found from *Figure C.14* found in *Appendix C*. As suggested in ANSI standards, the ratio of keyway radius over the diameter of the shaft r/d is usually kept to 0.021 for diameters below 6.5 inches. Assuming that the diameters which will be computed are going to be below this limit, the ratio was always kept this at 0.021, which resulted in a K_{ts} values of 3.0 and a K_t value of 2.2 for all keyways.

The mean-stress fatigue concentration factors can be computed next. For fluctuating stress, the mean component of stress is treated differently depending on the ductility of the material. There are three cases that must be verified to determine the value of k_{fm}. The three cases are summarized in equations (15) to (17) below:

$$\text{If } K_f\left|\sigma_{max_{nom}}\right| < S_y \text{ then: } K_{fm} = K_f \tag{15}$$

$$\text{If } K_f\left|\sigma_{max_{nom}}\right| < S_y \text{ then: } K_{fm} = \frac{S_y - K_f\sigma_{a_{nom}}}{|\sigma_{m_{nom}}|} \tag{16}$$

$$\text{If } K_f\left|\sigma_{max_{nom}} - \sigma_{min_{nom}}\right| > 2S_y \text{ then: } K_{fm} = 0 \tag{17}$$

In the first case no yielding occurs; in the second, local yielding occurs during the first cycle, limiting maximum stress to the yield stress; and in the third, irreversible yielding occurs. The first case is preferred since no yielding occurs and computations are much simpler.

For the shear stress due to torque, the same three cases apply with modifications: S_y is replaced by $S_{ys} = 0.577S_y$, $\sigma_{max_{nom}}$ by $\tau_{max_{nom}}$, and K_f by K_{fs}. $\sigma_{max_{nom}}$ and $\tau_{max_{nom}}$ are calculated by summing the corresponding equations (26) and (28) respectively without the safety factors.

II. Alternating and Mean Torque Components

Bending moments are determined from the bending moment diagram, while the mean and alternating torque components are calculated using the input shaft's power and rotational speed. Since torque and rotational speed for each shaft are constant, the mean and alternating components are derived using the following equations:

$$T_a = \frac{T_{max} - T_{min}}{2} \qquad T_m = \frac{T_{max} + T_{min}}{2} \tag{18}$$

In this current case, the $T_{max} = T_{min}$, hence alternating torque is zero for all shafts.

III. Endurance Limit and Correction Factors

The uncorrected endurance limit S'_e is the stress at the knee of a material's S-N curve. While some materials do not experience a knee, in which case the fatigue strength is used, steel exhibits a knee. Depending on the steel's ultimate tensile strength, the uncorrected endurance limit is equal to the following:

$$S'_e \cong 0.5S_{UT} \text{ for } S_{UT} < 200\ ksi \tag{19}$$

$$S'_e \cong 100\ ksi \text{ for } S_{UT} \geq 200\ ksi \tag{20}$$

These formulas give the uncorrected endurance limit and must therefore be modified to accommodate for differences between the test specimen and the actual part being designed. This is done by using correction factors which are presented below.

i. Loading effects

The data given in the textbook are for rotating bending tests. Therefore, if any other type of loading is applied on the part, the load correction factor will account for it. For bending and torque, the $C_{load} = 1$, and for axial loading $C_{load} = 0.7$.

ii. Size Effects

The data given in the textbook are based on the small rotating beam specimens. Thus, if the part is not cylindrical or if the diameter is bigger, the load factor will account for it. For a rotating cylinder, just like each shaft in this gearbox, the size factors are the following:

$$\text{for } d \leq 0.3\ in,\ C_{size} = 1 \tag{21}$$

$$\text{for } 0.3\ in\ < d\ \leq 10\ in,\ C_{size} = 0.869d^{-0.097} \tag{22}$$

iii. Surface Effects

The rotating beam test is done on a specimen which has been polished to a mirror like finish. However, real life parts will most likely not have this type of finish and the surface effect correction factor accounts for this. The material used for the shafts is cold rolled steel, and the correction factor can be computed with the following equation:

$$C_{surf} \cong A(S_{UT})^b \tag{23}$$

For cold rolled material and S_{UT} in MPa, as given by *Figure C.15* in *Appendix C*, constant $A = 4.51$, and constant $b = -0.265$.

iv. Temperature Effects

Fatigue tests are usually done at room temperature, but higher temperatures affect the material properties of the part. Therefore, the temperature correction factors account for this. For temperature smaller than 450℃, the $C_{temp} = 1$.

v. Reliability

The given data is usually a mean value which results from a scatter of multiple data. The reliability factor is given from *Figure C.16* given in *Appendix C* and depends on the assumed reliability. For aerospace components such as gearboxes, a reliability percentage of 99% is common and was therefore assumed, which resulted in a $C_{reliab} = 0.814$.

The corrected endurance limit can now be found and will be used to compute the diameter:

$$S_e = C_{load} \cdot C_{size} \cdot C_{surf} \cdot C_{temp} \cdot C_{reliab} \cdot S'_e \tag{24}$$

IV. Shaft Stresses

The following equations must be used at each critical location to find their respective stresses. The largest alternating and mean bending stresses can be found using equations (25) below:

$$\sigma_{a,b} = K_{f,b}\frac{M_a c}{I} \qquad \sigma_{m,b} = K_{fm,b}\frac{M_m c}{I} \tag{25}$$

Where $k_{f,b}$ and $k_{fm,b}$ are stress concentration factors, M_a and M_m are alternating and mean bending stress components respectively, c is the radial location of interest, and I is the first moment of inertia. Since the shafts designed are all cylindrical, the corresponding equations for c and I can be substituted in equation (25) above:

$$\sigma_{a,b} = K_{f,b}\frac{32M_a}{\pi d^3} \qquad \sigma_{m,b} = K_{fm,b}\frac{32M_m}{\pi d^3} \tag{26}$$

Where d is the diameter of the shaft at the desired location.

Now, the alternating and mean torsional shear stress components are found from the following equation:

$$\tau_a = K_{fs}\frac{T_a r}{J} \qquad \tau_m = K_{fsm}\frac{T_m r}{J} \tag{27}$$

Where k_{fs} and k_{fsm} are stress concentration factors, T_a and T_m are alternating and mean torque components, and J is the second moment of inertia. Substituting the corresponding r and J values for a solid round cylinder yields the following:

$$\tau_a = K_{fs}\frac{16T_a}{\pi d^3} \qquad \tau_m = K_{fsm}\frac{16T_m}{\pi d^3} \tag{28}$$

Where d is the diameter of the shaft at the desired location.

If there is any axial force on the shaft, it will typically only have a mean component, which means that it will be constant. The mean component of the axial stress can be found with the following formula:

$$\sigma_{m,axial} = K_{fm,a}\frac{F_z}{A} \tag{29}$$

Where A is the reduced area, and its formula can be replaced knowing that the designed shafts are cylinders

$$\sigma_{m,axial} = K_{fm,a}\frac{4F_z}{\pi d^2} \tag{30}$$

For shafts 1, 2, and 3 there were no axial loads, so equation (30) above can be set to zero. The Von Mises stress can now be computed with the axial force being zero:

$$\sigma'_a = \sqrt{\sigma_a^2 + 3\tau_a^2} \tag{31}$$

$$\sigma'_m = \sqrt{\sigma_m^2 + 3\tau_a^2} \tag{32}$$

V. Diameter

Now that all the above steps have been completed, iteration to find the diameters may begin. Since all the mean and alternating loads maintain a constant ratio in this context, the third case of failure model is used which is described by the following equation:

$$\frac{1}{N_f} = \frac{\sigma'_a}{S_e} + \frac{\sigma'_m}{S_{ut}} \tag{33}$$

In the case of shafts 1, 2 and 3, the axial load is zero. Thus, plugging equations (26), (28), (31), and (32) in the equation (33) above yields the following equation for the shaft diameter:

$$d = \left\{\frac{32N_f}{\pi}\left[\frac{\sqrt{(K_f M_a)^2 + 0.75(K_{fs}T_a)^2}}{S_e} + \frac{\sqrt{(K_{fm}M_m)^2 + 0.75(K_{fsm}T_m)^2}}{S_{ut}}\right]\right\}^{1/3} \tag{34}$$

The procedure for finding the diameter varied slightly from shaft to shaft because different critical points were analyzed. Thus, the paragraphs below will explain how the iteration process was conducted for each shaft.

i. Input shaft

Two critical locations are analyzed. The large diameter at gear 1 (D_1) was determined first using a safety factor of 1.75. This value was then fixed to iterate the smaller diameter d_1 at the shoulders, with a set fillet radius (r). During each iteration, new stress concentration factors were calculated to account for the changes in the D/d ratio. The final value of D_1 and d_1 will be presented in the *Results* section.

ii. Shaft 2 and 3

Five critical points were analyzed on shafts 2 and 3: three shoulders (between d_2 and D_2, between D_2 and D_3, and between D_3 and d_3.

First, the keyway at gear 2 was analyzed to determine D_2, following by determining D_3 at gear 3's keyway. With now D_2 and D_3 fixed, the middle shoulder was analyzed by assuming a fillet radius, then determining another value for the smaller of the two input diameters. If the first computed value for D_2 was bigger than this one, then the two major diameters were deemed safe.

The final two critical locations were solved using the same method as for shaft 1. For example, D_2 was set for the first shoulder, and with an assumed fillet radius, d_2 was iterated. The same approach was applied to d_3 and the bigger value of the two was set as the final dimensions for both d_2 and d_3.

3.2.6 Determination of Safety Factors Using Set Diameter (Shaft 4)

The procedure for the output shaft is a bit different than for the other shafts due to the presence of an axial load from the propeller. Indeed, equation (34) above can only be used on the assumption that the axial load is zero. Thus, another approach must be used since the diameter of the shaft can no longer be iterated for.

I. Stress Concentration Factors

For the output shaft, the stress concentration factors, and fatigue stress concentration factors are determined in the exact same way as for the other shafts, i.e. using *Figures C.10* to *C.12*. Though, $K_{t,a}$ will not be equal to zero in this case and, as a result, a $K_{f,a}$ and $K_{fm,a}$ will be computed. Again, the mean-stress concentration factors will be determined using shaft stresses that are computed later.

II. Alternating and Mean Torques

The alternating and mean torques are determined using equation (18) once again. Here, the maximum and minimum torque in shaft 4 are the same and are equal to the torque in the last shaft.

III. Endurance Limit and Correction Factors

This step is done the same way as in 3.2.5.

IV. Shaft Stresses

Just like for the previous shafts, at each critical point, the nominal alternating and mean stress components were determined for the bending and torsion in the shaft using equations (26) and (28). In this case, the critical points are the shoulders before and after gear 4, the keyway at gear 4, and bearing 6. Note that bearing 6 has been chosen as a critical location despite having no stress concentration due to the moment at this location being non-zero.

The nominal stress components of the axial load were computed using the following equations:

$$\sigma_{axial,max,nom} = \sigma_{axial,min,nom} = \frac{F_x}{A} = \frac{4F_x}{\pi d^2} \tag{35}$$

where A is the reduced area at the stress concentrator. Here, the maximum and minimum normal stresses are equal due to the axial load being constant. Then, the mean stress component was computed with the same relation used for the alternating and mean torques. Since $\sigma_{x,max} = \sigma_{x,min}$, there is no alternating stress component associated with the axial load.

Now that this is done, one can compute the combined nominal mean and alternating stress components with the following equations:

$$\sigma_{m,nom} = \sqrt{(\sigma_{m,b} + \sigma_{m,a})^2 + 3\tau_m^2} \tag{36}$$

$$\sigma_{a,nom} = \sqrt{(\sigma_{a,b})^2 + 3\tau_a^2} \tag{37}$$

The mean-stress fatigue concentration factors must be computed for the following components: $\tau_{max,nom}$ and K_{fs}, $\sigma_{max,nom}$ and K_f, and $\sigma_{max,nom}$ and $K_{f,a}$. Thus, using the same three cases presented as equation (15) to (17), the mean-stress concentration factors are determined for each load type. $\sigma_{max,nom}$ can be obtained by summing up equations (36) and (37), and $\tau_{max,nom}$ is obtained in the same manner as in 3.2.5.

Finally, the combined maximum mean and alternating stresses can be computed using equations (38) and (39) below. These consider the fatigue factors as opposed to equations (36) and (37).

$$\sigma_a' = \sqrt{\left(K_{f,b}\sigma_{a,b}\right)^2 + 3\left(K_{fs}\tau_{a,nom}\right)^2} \tag{38}$$

$$\sigma_m' = \sqrt{(K_{fm,b}\sigma_{m,b} + K_{fm,a}\sigma_{m,a})^2 + 3(K_{fsm}\tau_{m,nom})^2} \tag{39}$$

V. Diameter

When the axial load is nonzero, equation (33) is used instead of equation (34). For the output shaft, the analysis involves setting a diameter as input and calculating the safety factor. If the safety factor exceeds 1.75, the diameter is deemed safe.

Three critical locations are analyzed at the output shaft. First, the diameter at the keyway D_4 is determined. Next, D_4 and a fillet radius are fixed, and the shoulder fillet is analyzed. A small diameter d_4 is guessed, and its safety factor is computed. If the factor exceeds 1.75, d_4 is accepted; otherwise, the process is repeated until a new d_4 is found. Finally, d_4 is used to evaluate the safety factor at the last bearing

location. If the safety factor at the bearing exceeds 1.75, d_4 is approved. If not, a larger diameter is tested, ensuring that the safety factor determined earlier at the shoulder fillet does not decrease.

3.2.7 Standard Diameter Sizes for Shafts

The calculated shaft diameters were adjusted to align with standard machining values, as is standard engineering practice. Since there is no maximum budget allowed for this project, the exact values could have been used – at much higher machining costs – standard dimensions were chosen to simplify manufacturing and allow for standard bore diameters for gears and bearings.

For major diameters at gear locations, values were rounded up to the nearest $1/16$ inch (e.g., $1.03\ inches$ rounded to $1\ 1/16\ inches$). For smaller diameters at bearing locations, dimensions were rounded up to the nearest standard bearing bore diameter based on load requirements, using metric values from the SKF catalog.

3.2.8 Yield Failure

This report emphasizes fatigue failure but yield failure on the first cycle should still be considered. While the standard safety factor for the gearbox shaft is 1.75, a lower safety factor is deemed acceptable for yield failure. Given the unlimited budget for this gearbox, the shafts are assumed to be of very high quality with the material having little to no defects. A safety factor is a good measure of the risk of failure and how a material can behave under unpredictable circumstances. Yield failure is also most relevant during takeoff, where torque gradually increases to its maximum as the aircraft accelerates. The takeoff also makes up a small percentage of the plane's 2000-hour lifespan. Under these conditions, with high quality shafts and analysis based on maximum operating scenarios, a yield safety factor of 1.45 is considered sufficient for regular operation.

The yielding factor of safety can be computed using the following:

$$N_y = \frac{S_y}{\sigma_{max}} \tag{40}$$

where:

$$\sigma_{max} = \sigma_a + \sigma_m \tag{41}$$

Note that σ_a and σ_m are combined multiaxial stresses, i.e. they account for torsion, bending, and axial loads. In a real-life scenario, this factor would have to be considered when designing the gearbox, but due to the emphasis being placed on fatigue failure, this factor was computed but not considered to determine the shafts' dimensions.

3.3 Key Design

3.3.1 Design Background

Keys are crucial components in gearbox assemblies, enabling gears to rotate with the shafts. Comon key types include parallel keys (square or rectangular), tapered keys, and Woodruff keys. For this project, parallel keys were chosen due to their simplicity, ease of manufacturing and installation, and high torque capability. Since there was no requirement to prevent axial movement of gears along the shafts, tapered or Woodruff keys were unnecessary. Set screws and a hub on the gear, or snap rings could have been used to secure the gears in place, but there was no need to do so in this project.

Square parallel keys were designed based on standard US sizes provided in the course textbook (*Figure C.17* in the *Appendix*), which relates shaft diameter to key dimensions. Only a few parameters must be accounted for when designing a key. Indeed, the width is determined by the shaft diameter, the height by the width (for square keys), and the length is adjusted based on the desired safety factor.

3.3.2 Material Selection

To ensure keys fail first under shear loads – minimizing cost and simplifying replacement compared to failure of shafts or gears – a ductile material with a low elastic modulus and yield strength was selected. Square or rectangular parallel keys are typically made from cold-rolled steel bar stock, cut to the required length. Since the gearbox is assumed to be sealed and corrosion is therefore not a concern, AISI 1020 cold-rolled steel was chosen. Key material properties are summarized in *Table 5* below [4]:

Table 5: Material Properties of AISI 1020 Cold-Rolled Steel

Material	Density		S_y		S_{UT}		S_e	
	$[g/cm^3]$	$[lbs/in^3]$	$[MPa]$	$[psi]$	$[MPa]$	$[psi]$	$[MPa]$	$[psi]$
AISI 1020 Cold-Rolled Steel	7.87	0.2843	393	57 000	469	68 000	234.5	34 000

3.3.3 Safety Factor Calculations

Three safety factors must be found when designing keys and keyways. The first one being the safety factor of the shaft at due to the stress concentration caused by the keyway. This is already done in the *Shaft Design* section and must not be done once again here. The two other safety factors that need to be found are the following: the safety factor against bearing failure N_s and against fatigue failure N_f.

I. Safety Factor Against Bearing Failure

The safety factor against bearing failure is given by the following equation:

$$N_s = \frac{S_y}{\sigma_{max}} \tag{42}$$

Where S_y is the yield strength of the material, and σ_{max} is the bearing stress on the key given by the equation below:

$$\sigma_{max} = \frac{F_m + F_a}{A_{bearing}} \tag{43}$$

Where F_m is the mean force component, F_a is the alternating force component, and $A_{bearing}$ is the bearing area. For a square cross-section parallel key, the bearing area is equal to the following:

$$A_{bearing} = \frac{H}{2} \times L \tag{44}$$

Where H is the key height and L is the key length. The mean and alternating components of force are given be the following equations:

$$F_a = \frac{T_a}{r} \qquad F_m = \frac{T_m}{r} \tag{45}$$

Where T_a and T_m are the alternating and mean torque components respectively, and r is the radius of the shaft at the key location.

II. Safety Factor Against Fatigue Failure

The safety factor against fatigue failure can be computed, for case 3, with equation (33) above with S_{UT}, the ultimate tensile strength of the material, S_e the corrected endurance limit, and σ'_a and σ'_m, the alternating and mean components of the Von Misses equivalent stresses respectively. They are given by the equation below.

$$\sigma'_a = \sqrt{\sigma_{x,a}^2 + \sigma_{y,a}^2 - \sigma_{x,a}\sigma_{y,a} + 3\tau_{xy,a}^2} \tag{46}$$

$$\sigma'_m = \sqrt{\sigma_{x,m}^2 + \sigma_{y,m}^2 - \sigma_{x,m}\sigma_{y,m} + 3\tau_{xy,m}^2} \tag{47}$$

For all the keys designed, the bending and axial stresses are null. The shear stress components are found from the following equations:

$$\tau_a = \frac{F_a}{A_{shear}} \qquad \tau_m = \frac{F_m}{A_{shear}} \tag{48}$$

Where F_a and F_m are once again the alternating and mean components of force and are given by equation (45) above, and A_{shear} is the shear area given by the equation below:

$$A_{shear} = W \times L \tag{49}$$

Where W is the width of the key and L is the length.

The minimum safety was set to 1.5 for keys 2, 2', 3, and 3', and was set to 1.6 to for keys 1 and 4. This approach ensures that if a key on shaft 2 or 3 fails, the other intermediate shaft may remain operational. While the project did not analyze whether the gearbox could function with only one intermediate shaft transmitting torque, such analysis would be necessary in a real world-application. This design decision aims to maintain gearbox operability in the event of a key failure.

3.4 Bearing Selection

3.4.1 Types of Bearing

After determining the shafts diameters, the bearing selection process began, as the shaft diameter dictates the bearing bore size. The type of bearing was selected based on the applied loads, which vary for each shaft. The main bearing types analyzed were as follows:

I. Journal Bearings

This type of bearing is usually suitable for heavy loads and low to moderate speed applications. They require constant lubrication, and would therefore require a lubrication system, and they cannot fully resist axial loads.

II. Rolling Element Bearings

Two main types of rolling element bearings that were analyzed are ball and roller bearings.

i. Ball Bearings

Ball bearings are ideal for low to moderate loads and high-speed applications due to their low friction and small contact area. Some designs can handle both radial and axial loads, although they are stronger in the radial direction.

ii. Roller Bearings

With larger radial contact areas, these bearings are suited for heavier loads, but lower operational speed due to their higher friction. Some designs like the one that will be discussed just below are suitable for both radial and axial loads. Again, some types of roller bearings are suitable for axial load due to the shape of the rolling elements. Roller bearings are usually heavier and take up more space than ball bearings.

iii. Tapered Roller Bearings

These bearings use angled rollers to provide high contact area in both the radial and axial directions, making them appropriate for moderate to high loads in both directions. They are, however, suitable for low to moderate speed applications.

iv. Thrust Bearings

Thrust bearings are designed for axial loads only. They cannot handle any radial loads and must be paired with another bearing type if radial loads are present.

For this project, rolling element bearings were chosen over journal bearings since they do not require regular maintenance for the lubricant, have lower friction which has a direct influence on power losses, and have better load capacity axially. For the first two bearings on shaft 1, regular ball bearings were chosen, same for each of the two bearings on shaft 2 and 3. For shaft 4 however, a tapered roller bearing was chosen to handle the axial load created by the propeller, alongside a regular ball bearing.

3.4.2 Bearings' Required Life

The bearing analysis is based on required lifespan, measuring in millions of revolutions, rather than a safety factor unlike other gearbox components. The required lifespan is calculated by multiplying the shaft's angular velocity by the component's total operational duration, which is 2000 hours in this case.

3.4.3 Bearing Life Analysis

The first step of the bearing analysis is to determine the axial and radial support reactions at each bearing. Axial reactions only apply to the output shaft, as it is the only shaft under axial load. Thus, either support 5 or 6 must have a reaction in this direction, though an alternative approach could distribute the axial reaction forces between both bearings.

I. Input Shaft and Shaft 2 & 3

The procedure for these shafts is the same since they have no axial loads. The input shaft having symmetrical loads, both bearings will thus be the same. Though, for shafts 2 and 3, since the bending moment at support 4 is greater than at support 3, the bearing design at 4 safely be applied to support 3. This approach ensures simplicity as well as safety in the design.

The resulting radial force at a bearing location is then given by:

$$F_r = \sqrt{R_{i,y}^2 + R_{i,z}^2} \tag{50}$$

where the subscript i represents a given support location, y represents the y-axis in the wings' direction, and z represents the z-axis in the vertical direction. In this gearbox, there is no reaction force in the y-axis for any shaft, so the radial force is always equal to the vertical reaction. Again, axial forces are not considered for shafts 1,2, and 3. Then, based on the small shaft diameters determined in the shaft analysis, appropriate bearing bore diameters can be selected. The final bearing choice should also account for dynamic and static load ratings, as well as speed ratings, hence ensuring the bearing can handle the required loads and rotational speeds.

Bearings for the gearbox were selected from the SKF catalogue which offers a wide variety of bearings suited for multiple applications [5]. Once a bearing is chosen, a reliability factor must be chosen. Here, a reliability factor of 90% was chosen, corresponding to a coefficient $K_R = 1$. This factor was chosen since the L_{10} life of a bearing is a standardized value for many applications. While higher reliability factors are required in commercial aircraft for passenger safety, the Solar Impulse plane, being a single-seat aircraft focused on endurance and performance, justifies the use of this reliability factor. Thus, the actual bearing life for ball bearings is found using the following:

$$L_{10} = \left(\frac{C}{P}\right)^3 \tag{51}$$

where C is the dynamic rated loading and P is the radial load in this case. If the L_{10} value computed exceeds the required life, then the bearing is suitable. Note that several bearings were tried before finding those that will be presented in the *Results* section.

II. Output Shaft

The procedure for shaft 4 is a bit more complicated due to the presence of an axial load. As before, the radial forces at both bearing locations are determined from the FBDs, and the axial force is given as $F_a = 1000lbf = 4448N$. It was decided that only bearing 6 will be responsible for countering this force while bearing 5 is designed like the others.

The radial force for bearing 6 is determined using equation (50) above and the axial force magnitude is known. First, a bearing is first selected, and the ratio F_a/C_0 is determined. Then, the factor e is interpolated using *Appendix C.18*. Next, we check if F_a/VF_r is greater or lower than e with $V = 1$ since the inner ring is rotating. Based on the result of the inequality, X and Y coefficients can be interpolated from *Appendix C.18*. These coefficients are used to subsequently compute an equivalent load P that accounts for both axial and radial loads using equation XX below.

$$P = XVF_r + YF_a \tag{52}$$

Finally, the equivalent load P is substituted in equation (53) below, giving the L_{10} life for roller bearings:

$$L_{10} = \left(\frac{C}{P}\right)^{10/3} \tag{53}$$

This value is then compared to the required life.

3.4.4 Other Selection Criteria

As noted earlier, the L_{10} life is the primary factor in determining a bearing's suitability for the gearbox. However, additional criteria were considered, including reference speed, which depends on thermal conditions at operating temperatures, and limiting speed, which reflects the mechanical limits of the bearing components [6].

4. Results

The final solution for the gearbox is presented below in *Figure 4* and the corresponding assembly drawing is presented in *Appendix H*. Drawings for the output shaft 4 and for gear 4 are also presented in this Appendix, along other views of the gearbox assembly.

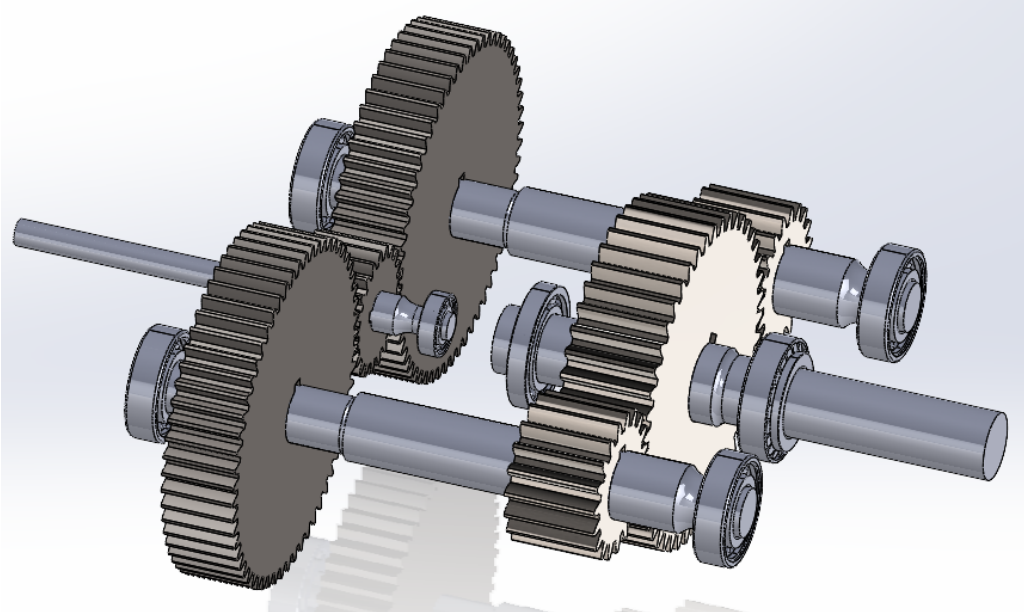

Figure 4: Final Gearbox Design for Solar Impulse Plane

4.1 Gear Analysis

4.1.1 Gear Geometric Parameters

From the analysis and optimization discussed in the previous sections, the selected gear teeth combination as well as the geometric parameters (pitch diameters, addendum, dedendum, face width, pitch circle) are tabulated in *Table 6* below. The sample calculations for these values and gear teeth number are presented in *Appendix D.3* and *D.5*.

Table 6: Selected Gear Teeth Combination and Gear Geometric Parameters

	Gear 1	Gear 2 & 2'	Gear 3 & 3'	Gear 4
Classification	Input gear	Reduction gear	Reduction gear	Output gear
Number of teeth	21	59	19	45
Diametral pitch [teeth/in]	10	10	8	8
Pitch circle [teeth/in]	0.3142	0.3142	0.3927	0.3927
Addendum [in]	0.1	0.1	0.125	0.125
Dedendum [in]	0.125	0.125	0.15625	0.15625
Face width [in]	1.3	1.3	1.625	1.625

4.1.2 Material

According to the selection criteria presented in the *Theoretical Development* section and the material properties shown in *Appendix D.9* [2,7,8], the following material combinations have been tested during the iteration process for the load and stress analysis presented later:

I. Gearset 1 (Gear 1 and Gear 2)
   i. Steel Pinion-Cast Iron Gear
      This pair of materials fail since the safety factor for surface failure for gears 3 and 4 are lower than 1.5.
   ii. Steel Pinion-Steel Gears
      This pair of materials meets the design requirement but is heavier than the pair of material that was chosen.
   iii. Ti-6Al-4V Pinion-Ti-6Al-4V Gears (Final Choice)

In the final trial, the titanium alloy Ti-6Al-4V was chosen for both pinion and gears due to its exceptional strength-to-weight ratio and density 43% lower than steel at 4.5 g/cm^3. This significantly reduces gearset weight while maintaining structural integrity. It also offers great fatigue strength, ideal for weight-sensitive, high-performance applications. The analysis confirmed a minimum safety factor above 1.5 for both components, ensuring reliability under operational stress, making Ti-6Al-4V the optimal choice for Gearset 1.

II. Gearset 2 (Gear 3 and Gear 4)

The second stage of a 2-stage reduction gearbox endures higher torque and workload due to the additional speed reduction. As torque increases proportionally to the reduction ratio, tooth stress also rises. Thus, the second-stage pinion and gear must be at least as strong as those in the first stage to withstand the increased stresses without failure.

i. Ti-6Al-4V Pinion-Ti-6Al-4V Gear

This pair of material fails since the safety factor for surface failure for gears 3 and 4 are lower than 1.5.

ii. Steel Pinion-Ti-6Al-4V Gear

This pair of material fails since the safety factor for surface failure for gear 4 is lower than 1.5.

iii. Steel Pinion-Steel Gear (Final choice)

In the final trial, steel was selected for both the gear and pinion due to its superior strength, toughness, and hardness. This choice increased the second-stage safety factor well above the minimum of 1.5. Although heavier than titanium, steel's strength ensured reliability and durability under the higher stresses of the second stage, making it the optimal material for this application.

Material selection must reflect the stress conditions of each gearbox stage. Ti-6Al-4V, with its strength, hardness, and low density, was ideal for Gearset 1, handling first-stage stresses while minimizing weight. For Gearset 2, subjected to higher torque and workload, steel was chosen for its superior strength to ensure safety and reliability. Key material properties for both materials are presented below in *Table 7*.

Table 7: Material Properties of Chosen Materials for the Gears

Material	Density [g/cm^3]	Elastic modulus [$kpsi$]	Fatigue Strength [psi]	Hardness [HB]
AISI 4340 steel (Nitrided)	7.85	29000	50800	552
Titanium alloy (Ti-6Al-4V)	4.5	16510	87000	336

4.1.3 Torque Analysis

According to equation (2), the torque in each shaft can be computed which will provide the torque experienced in each gear of both gear sets. These torques are summarized in *Table 8* below, and a sample calculation is shown in *Appendix D.6*.

Table 8: Torque Experienced in Each Shaft

Shaft	Torque [$lb \cdot ft$]	Torque [$N \cdot m$]
Shaft 1	57.30	77.68
Shaft 2 & 3	160.97	218.25
Shaft 4	381.25	516.91

Note that since the torque applied is constant, these torques correspond to the magnitude of both the maximum and minimum torque values. Also, the torque experienced by pinion 1 (gear 1) is that of shaft 1, and the torque experienced by pinion 2 (gear 3) is that of shaft 2.

4.1.4 Load and Stress Analysis

The detailed process to compute transmitted loads is presented in *Appendix D.6*. The calculation results are shown below in *Table 9*.

Table 9: Load Parameters for Gearsets

	T_p	W_t
Gearset 1	687.55 $lb \cdot in$	327.40 lb
Gearset 2	1931.69 $lb \cdot in$	813.34 lb

Note that the W_t values presented have been divided by 2 since there is symmetry in the gearbox. For instance, gear 1 transmits its torque to both gear 2 and 2' resulting in the transmitted load being half of the calculated value.

Gearset 1

Following the process introduced in the theoretical development for gears, the values of correction factors in gearsets are calculated and listed in *Table D.10.1* to *D.10.4* in *Appendix D.10*. Then substitute all the values in corresponding equations, each stress and safety factor can be obtained, which are summarized in *Table 10* below. The detailed process of calculation for gearset 1 is provided in *Appendix D.10*.

Table 10: Summarized Values of Stress Analysis for Gearset 1

Parameters	Gearset 1	Gearset 2
$\sigma_{b,p}$ $[psi]$	13300.92	26457.93
$S_{fb,p}$ $[psi]$	50132.44	88235.53
$\sigma_{b,g}$ $[psi]$	11276.79	22405.81
$S_{fb,g}$ $[psi]$	51521.91	88718.72
σ_c $[psi]$	78642.23	157734.59
$S_{fc,p}$ $[psi]$	138788.38	264148.62
$S_{fc,g}$ $[psi]$	145525.14	266661.53
$\boldsymbol{N_{b,p}}$	**3.769**	**3.335**
$\boldsymbol{N_{b,g}}$	**4.569**	**3.960**
$\boldsymbol{N_{c,p}}$	**1.765**	**1.675**
$\boldsymbol{N_{c,g}}$	**1.850**	**1.691**

The stress analysis for gear sets 1 and 2 highlights safety factors and potential failure modes in the gearbox design. For Gearset 1, the lowest safety factor, $N_{c,p} = 1.765$, occurs in the pinion due to contact stress, making it the most vulnerable component of the two. This suggests a higher likelihood of surface fatigue or pitting over time or under extreme load conditions. Bending stresses have higher safety factors and are less critical by comparison, with contact stress in the pinion being the primary concern for durability.

For gearset 2, the minimum safety factor, $N_{c,p} = 1.674$, also arises from contact stress in the pinion. Safety factors for Gearset 2 are slightly lower than those for Gearset 1, indicating a higher susceptibility to failure, particularly in the pinion. Thus, the pinon in Gearset 2 is the most critical component across both gearsets, with surface fatigue and pitting being the primary risks.

4.1.5 Gear Train Weight Estimation

Gear weight is a critical factor in total gearbox weight and is essential for design and optimization, particularly in aerospace applications where minimizing weight enhances performance. To estimate gear weight, each gear is approximated as a cylinder with a diameter equal to its pitch diameter and height equal to its face width. This simplification enables quick weight calculation.

As detailed earlier, the first gearset uses a titanium alloy, and the second gearset uses AISI 4030 nitrided steel. Gear weights are calculated using the respective material densities, pitch diameter, and face widths. The calculated weights of all individual gears are presented in *Table 11* below. The total weight of the gears is 12620.65 g.

Table 11: Weight of The Gears and Pinions in the Gearbox Design

	Gear 1	Gear 2 and 2'	Gear 3 and 3'	Gear 4
Gear material	Titanium alloy	Titanium alloy	AISI 4340 steel	AISI 4340 steel
Face width [in]	1.3	1.3	1.625	1.625
Estimated volume [cm^3]	73.786	582.423	117.970	661.743
Estimated weight [g]	332.04	2620.90	926.07	5194.68

The weight estimation made using the method shown above will overestimate the results since it does not consider the holes and keyways to fit the shafts and keys. To obtain a more precise weight estimation, the volumes of the gears are calculated using CAD software. The weight estimation obtained from SolidWorks is presented in section *4.5* below. This weight estimation was used in the shaft design process.

4.2 Shaft Results

4.2.1 Material Selection

All gearbox shafts are made from cold-rolled AISI 1045 steel, selected for its excellent strength-to-weight ratio and superior strength due to its carbon composition. Cold-rolled steel was chosen over hot-rolled steel because the small shaft sizes result in higher stress levels, and cold-rolled materials tend to have higher strength. The material properties of this steel are summarized in *Table 3* presented in section *3.2.2*.

4.2.2 Stress Concentrators

As discussed earlier, the gearbox design includes two stress concentrators: keyways and shoulders. A general shaft geometry is shown in *Figure 3*. Shoulder and keyway radii were determined during diameter iteration and will be presented later in the analysis.

4.2.3 FBDs and Shear & Bending Moment Diagrams

Multiple FBD configurations were created to explore different shaft lengths, with the final designs presented in *Appendix E.1*. Initial dimensions were estimated to complete the FBDs and begin shaft analysis. To streamline the process, the distance between the two bearing centers for each shaft was fixed throughout the iterations.

I. Input Shaft 1
The bearing distance was set to $87.3075\ mm$.

II. Output Shaft 4
The bearing distance was set to $109.85\ mm$ to accommodate higher loads and larger bearings.

III. Shafts 2 and 3
Bearing distance was initially set at $241.2075\ mm$, which was determined by aligning the gearsets and allowing an initial space of $2.5\ cm$ between the input and output shafts. This value was adjusted when the shafts length changed during the design process.

For all shafts, a $10\ mm$ clearance was maintained on each side of the gears, and the bearing-to-shoulder distance depended on the width of the bearings and the total length between the two bearing centers. Shaft 4 includes a $10\ cm$ extrusion measured from the bearing center to install the propeller. The gear weights used to design the shafts were estimated in section *4.1.5*. Although this approach was not optimized, fixing bearing distances saved time.

Shear and bending moment diagrams were constructed for each shaft and are presented in *Appendix E.2* as *Figure E.2.1*, with calculations for Shaft 1 provided as a sample in *Appendix E.2*. From these diagrams and known dimensions of stress concentrators, maximum bending moments were calculated for critical locations and are summarized in *Table 12*.

Table 12: Bending Moments at Critical Locations for Shafts 1 to 3

Shaft 1	Shaft 2	Shaft 3

Critical Location	Bending Moment $[N \cdot m]$	Critical Location	Bending Moment $[N \cdot m]$	Critical Location	Bending Moment $[N \cdot m]$
Shoulder Fillet 1	0.0279	Shoulder Fillet 3	-7.87	Keyway 4	-47.91
Keyway 1	0.0576	Keyway 2	-12.66	Shoulder Fillet 7	-75.79
–	–	Shoulder fillet 4	26.09	Max Bending Moment	-98.10
–	–	Keyway 3	111.69	–	–
–	–	Shoulder Fillet 5	221.68	–	–

For Shaft 1, only one shoulder fillet was analyzed due to symmetry, as both are identical. Similarly, for Shaft 4, only the fillet with the worst bending moment was analyzed, ensuring the other is also safe. Additionally, the maximum bending moment on Shaft 4, located between bearing 6 and the shaft end, was analyzed separately, as it does not coincide with a stress concentrator.

4.2.4 Stress Concentration Factors

The stress concentration factors, fatigue stress concentration factors, and mean-stress concentration factors for all the critical locations given above are given in *Table 13* and *14* below. Note that all these factors were found based on the determined diameters for each shaft that will be presented further in this report. Furthermore, a sample calculation for these factors is given in *Appendix E.3*.

Table 13: Stress Concentration Factors for Shaft 1, 2, and 3

Shaft	Location	K_t	K_{ts}	K_f	K_{fs}	K_{fm}	K_{fsm}
Shaft 1	Shoulder Fillet 1	0.931	0.835	0.937	0.847	0.937	0.847
	Keyway 1	2.2	3.0	1.751	2.360	1.751	2.360
Shaft 2 & 3	Shoulder Fillet 3	1.033	0.921	1.030	0.927	1.030	0.927
	Keyway 2	2.2	3.0	1.806	2.445	1.806	2.445
	Shoulder Fillet 4	1.611	1.337	1.499	1.287	1.499	1.287
	Keyway 3	2.2	3.0	1.828	2.478	1.828	2.478
	Shoulder Fillet 5	1.079	0.959	1.072	0.962	1.072	0.962

Table 14: Stress Concentration Factors for Shaft 4

	Location	$K_{t,a}$	$K_{t,b}$	K_{ts}	$K_{f,a}$	$K_{f,b}$	K_{fs}	$K_{fm,a}$	$K_{fm,b}$	K_{fsm}
Shaft 4	Keyway 4	1.482	1.436	1.199	1.417	1.377	1.177	1.417	1.377	1.177
	Shoulder Fillet 7	2.2	2.2	3.0	1.848	1.848	2.509	1.848	1.848	2.509
	Bearing 6	N/A	N/A	N/A	N/A	N/A	N/A	N/A	N/A	N/A

4.2.5 Corrected Endurance Limits

For every shaft diameter in the gearbox, a corrected endurance limit had to be computed to account for varying C_{size} values along the shaft. Sample calculations for the uncorrected endurance limit, correction factors, and the corrected endurance limits, along with a summary table, are provided in *Appendix E.4*.

4.2.6 Shaft Stresses

Using the methodology and equations from the *Theoretical Development* section, the maximum stresses at each critical location are calculated and summarized in *Table 15*, incorporating fatigue concentration factors. For shafts 1 to 3, the σ_{max} values represent bending stresses, while shaft 4 includes two values. A sample calculation is provided in *Appendix E.5* and *E.6*.

Table 15: Maximum Stresses at Each Critical Locations

Shaft	Location	σ_{max} [MPa]		τ_{max} [MPa]
		Bending	Axial	
Shaft 1	Shoulder Fillet 1	0.164	–	206.733
	Keyway 1	0.227	–	206.623
Shaft 2 & 3	Shoulder Fillet 3	14.384	–-	179.277
	Keyway 2	15.154	–-	176.820
	Shoulder Fillet 4	22.348	–	93.043
	Keyway 3	82.896	–	109.800
	Shoulder Fillet 5	49.502	–	109.770
Shaft 4	Keyway 4	227.404	227.404	160.833
	Shoulder Fillet 7	286.048	294.367	120.721
	Bearing 6	246.697	246.697	116.770

Notice that for shaft 4, there is only one axial maximum stress provided. This is because *Appendix C.14* provides only one value of K_t for keyways, thus this value is used for both bending and axial load. As for bearing 6, there is no stress concentrator at this point meaning that $K_f = K_{f,axial}$ resulting in only one value.

As mentioned earlier, the usual equation used to iterate for the diameter cannot be used for shaft 4 due to the presence of an axial load. For this reason, equation (33) must be used. Therefore, the maximum alternating and mean complex multiaxial stress components are computed and presented in *Table 16* below. The calculation for these is presented in *Appendix E.6*.

Table 16: Maximum Alternating and Mean Complex Multiaxial Stresses in Output Shaft 4

Location	σ'_a [MPa]	σ'_m [MPa]
Keyway 4	41.394	209.298
Shoulder Fillet 7	21.968	278.709
Bearing 6	44.322	202.376

Using the above values, the following safety factors are obtained for the final diameter values:

Table 17: Safety Factors for the Output Shaft 4 Using Final Diameter Dimensions

Location	N_f
Keyway 4	1.76
Shoulder Fillet 7	1.77
Bearing 6	1.76

The sample calculation for these factors is provided in *Appendix E.8*.

4.2.7 Final Shaft and Stress Concentrators Dimension

The final shaft dimensions and their corresponding standard sizes are presented in *Table 18*. All related stress concentrator dimensions are presented below in *Table 19*. Refer to *Figure E.1* in the *Appendix* to see to which dimensions the diameters are associated with. Note that the standard dimensions for minor diameters are found in millimeters due to the bearings being chosen in the SKF metric catalogue, and the dimensions for major diameters are found in inches due to the gears being designed following the AGMA standards. A sample calculation for calculating the diameters is provided in *Appendix E.7*.

Table 18: Final Shaft Dimensions

Shaft	Diameter	Obtained Value		Standard Dimension	
		[mm]	[in]	[mm]	[in]

Shaft 1	Minor Diameter d_1	11.75		**12.00**	
	Major Diameter D_1		0.6508		**11/16**
Shaft 2 and 3	Minor Diameter d_2	17.91		**22.00**	
	Major Diameter D_2		0.9787		**1**
	Major Diameter D_3		1.1524		**1-3/16**
	Minor Diameter d_3	21.36		**22.00**	
Shaft 4	Minor Diameter d_4	29.5		**30.00**	
	Major Diameter D_4		1.3583		**1-3/8**

Table 19: Final Stress Concentrator Dimensions

Shaft	Stress Concentrator	Obtained Value [mm]	**Standard Dimension** [mm]
Shaft 1	Shoulder Fillet Radius (1) & (2)	12.7	**12.70**
	Keyway (1) Fillet Radius	0.347193	**0.3667125**
Shaft 2 & 3	Shoulder Fillet (3) & (5)	12.7	**12.70**
	Keyway (2) Fillet Radius	0.522165	**0.5334**
	Shoulder Fillet (4)	2.5	**2.50**
	Keyway (3) Fillet Radius	0.614712	**0.6334125**
Shaft 4	Shoulder Fillet (6) & (7)	5	**5.00**
	Keyway (4) Fillet Radius	0.7245	**0.733425**

The "standard dimensions" in *Table 19* above are simply the stress concentrator dimensions associated with the standard dimensions presented in *Table 18*. The obtained values presented above yield safety factors of 1.75 or more everywhere along the shafts. By rounding up to the nearest value, the final safety factors for the shafts are all above 1.75, ensuring a reliable gearbox design.

4.2.8 Static Failure

As mentioned, static failure was considered in the new gearbox design with a desired safety factor of 1.45. This value was determined on the assumption that the shafts manufactured would be of high quality due to unlimited budgets and that this safety factor would be much higher if normal operating conditions were used instead of maximum operating conditions. The procedure to compute the yielding safety factors is provided in *Appendix E.9* along with a table summarizing the factors for every shaft.

Table E.9.1 in *Appendix E.9* shows that the smallest yielding safety factor is 1.48 which exceeds the 1.45 threshold. Although this is slightly below the typical 1.5 standard in the aerospace industry, it is still acceptable due to the assumptions presented earlier. Therefore, there is much certainty that the shafts will not fail under static loading on the first cycle.

4.3 Key Results

4.3.1 Geometry

Based on the shaft diameters, key geometry was determined using the "Standard Key and Setscrew Sizes for Metric Sized Shafts" table from the textbook, shown in the *Appendix* as *Figure C.17*. Geometry parameters for each key are listed in *Table 20* below.

Table 20: Designed Key Geometry

Key location	**Key 1**	**Key 2 and 2'**	**Key 3 and 3'**	**Key 4**
Shaft diameter [in]	0.6875	1	1.1875	1.375
Key width [in]	0.187	0.25	0.25	0.312
Key height [in]	0.187	0.25	0.25	0.312
Key length [in]	0.6	0.8134	0.685	1.004
Face width [in]	1.3	1.3	1.625	1.625

A square parallel key was selected for ease of manufacturing and installation. Key lengths were determined based on the safety factors outlined in section *4.3.4*, with notch radii detailed in the previous *Results* section.

4.3.2 Material Selection

As discussed, keys require a ductile material to fail first under shear, protecting other gearbox components. AISI 1020 cold-rolled steel was selected, with key material properties provided in *Table 5* of the *Theoretical Development* section.

4.3.3 Correction Factors

The correction factors to find the corrected endurance limit are determined based on the geometry and load conditions of the keys. The detailed computation process is shown in *Appendix F.1*, and the results are summarized in *Table F.1.2* in *Appendix F*.

4.3.4 Safety Factors

Key design considers shear fatigue failure and bearing failure. The safety factors are obtained by the equations introduced in the theoretical background part, and the results are shown in *Table 21* below. Sample calculations for these factors are shown in *Appendix F.1* and *F.2* Key lengths were set to achieve a minimum safety factor of 1.6, 1.5, 1.5, and 1.6 for keys 1, 2, 3 and 4 respectively. The reasoning behind this design decision is presented in the *Theoretical Development* section *3.3.3*.

Table 21: Safety Factor for Different Keys

Safety Factors	Key 1	Key 2 and 2'	Key 3 and 3'	Key 4
N_f	2.202	2.066	2.066	1.848
N_s	1.60	1.50	1.50	1.6

4.4 Bearing Results

4.4.1 Types of Bearings

As mentioned, the gearbox design includes two types of bearings: ball bearings (for bearing 1 to 5), and a tapered roller bearing for bearing 6. Ball bearings were selected for bearings on shafts 1,2 and 3 due to the moderate loads and rotational speeds experienced by these shafts, making ball bearings an obvious choice. For the output shaft, a ball bearing was used at support 5, while a tapered roller bearing was used at support 6. The tapered roller bearing was selected to handle the axial load from the propeller, while also supporting radial loads. Its larger surface of contact allows it to efficiently handle axial loads and distribute them more safely than ball bearings. As specified, in such configuration, only bearing 6 handles the axial load.

4.4.2 Bearings' Required Life

The procedure to determine each bearing's required life was already detailed in the *Theoretical Development* section and a sample calculation is provided in *Appendix G.1*. *Table 22* presents the required life for bearings based on the shaft they are located on.

Table 22: Require Life for the Gearbox's Bearings Based on Their Shaft

Shaft	Require life [10^6 revolutions]
Input (1)	660.00
2 & 3	234.92
Output (4)	99.19

4.4.3 Bearing Selection

The next step in the bearing analysis is to determine the L_{10} life based on various bearings until this value exceeds the required life presented above. A sample calculation is provided for this in *Appendix G.2* along with other parameters of the selected bearings such as dynamic and static load ratings. Once this is done, the bearings for the final gearbox design are determined and presented in *Table 23* below.

Table 23: Final Bearings Selected from the SKF Catalogue

Bearing Location	Type	Designation from SKF	L_{10} $[10^6 revolutions]$	Reference Speed $[RPM]$	Limiting Speed $[RPM]$
Bearing 1 & 2	Ball	6001	36,460,111,358	60,000	38,000
Bearing 3 & 4	Ball	63/22	260.055	28,000	18,000
Bearing 5	Ball	16006	2,580.764	28,000	17,000
Bearing 6	Tapered Roller	32006 X	336.022	10,000	12,000

**The selected bearings can be found at: https://www.skf.com/us/products/rolling-bearings (see *Reference* section: [5])

From the above table, we see that the selected bearings are appropriate based on their life, reference speed, and limiting speed since the maximum RPM experienced in the gearbox is $5500\ RPM$ which is well below the above speeds. A picture of the selected bearings with their respective specifications is presented in *Appendix G.3*.

4.5 Final Weight Analysis and Size Analysis

The final weight analysis was conducted using the CAD models. Indeed, once the final dimensions were established and the CAD models finalized, the SolidWorks mass properties tool was used to calculate each part's volume. As for the bearings, their mass is specified on the SKF website. *Table 24* below presents the volume of each part of the gearbox and their respective weight which were computed using the materials' density.

Table 24: Volume and Weight of Each Part of the Assembly

Component	Volume/component	Density	Number of Components	Weight/component	Weight
	$[mm^3/comp.]$	$[g/cm^3]$		$[kg/comp.]$	$[kg]$
Bearing 1 & 2	N/A	N/A	2	0.0195	0.039
Bearing 3 & 4	N/A	N/A	4	0.117	0.468
Bearing 5	N/A	N/A	1	0.085	0.085
Bearing 6	N/A	N/A	1	0.170	0.170
				Subtotal for Bearings	**0.762**
Shaft 1	18 297.26	7.85	1	0.1436	0.1436
Shaft 2 & 3	166 455.81	7.85	2	1.307	2.6133
Shaft 4	110 487.81	7.85	1	0.8673	0.8673
				Subtotal for Shafts	**3.624**
Gear 1	62 888.30	4.5	1	0.2830	0.2830
Gear 2	558 340.25	4.5	2	2.512	5.025
Gear 3	83 201.83	7.85	2	0.6531	1.306
Gear 4	611 361.46	7.85	1	4.799	4.799
				Subtotal for Gears	**11.413**
Key 1	341.03	7.87	1	0.002684	0.002684
Key 2	825.13	7.87	2	0.006494	0.01298
Key 3	691.55	7.87	2	0.005442	0.01088
Key 4	1583.00	7.87	1	0.01246	0.01246
				Subtotal for Keys	**0.0390**
				Total Weight of the Gearbox	**15.839**

The total weight of the gearbox is therefore $15.389\ kg$, exceeding the target weight of $5.5\ kg$ by around $10\ kg$. As shown in the above table, gears are the heaviest components of the gearbox. Therefore, any additional efforts at reducing weight should be concentrated on gears as they account for 72% of the total weight. Additionally, the weight table does not include the extrusion from shafts 1 and 4 connecting to the motor and propeller, as they are technically not considered part of the gearbox.

The exact size of the gearbox can also be determined from the finalized CAD model of the gearbox assembly. The final sizes are shown in *Table 25* below. Note that the length in the flight direction (x-direction) was measured from the first bearing to the furthest point of the last bearing.

Table 25: Final Sizes of the Gearbox Assembly

Direction	Size Limits [cm]	Actual Size [cm]
Flight Direction ($x-$)	30	**25.609**
Wing Axis ($y-$)	45	**35.814**
Vertical Axis ($z-$)	45	**15.494**

The designed gearbox then respects the size constraints.

4.6 General Tolerancing

No budget was specified for this project; hence we assumed that we had an unlimited budget to design the gearbox. Hence, we assumed that all the pieces would be machined with a very high degree of precision. More precisely, it was assumed that all parts could be machined with a tolerance of $\pm 0.0001\ in$ which is attainable with very high precision machines [9]. Of course, this would exponentially increase the cost of machining the parts and would probably not be an ideal choice in a real-life scenario. Similarly, for parts with angular dimensions, a tolerance of $\pm 0.01°$ was set. This tolerancing is displayed on the drawings.

5. Conclusion

The primary objective of this project is to design a lightweight, efficient two-stage reduction gearbox for a solar-powered aircraft, meeting requirements for dimensions, endurance, reduction ratio, safety factors, and failure order of mechanical components. The design focuses on four key components, designed in this order: gears, shafts, keys, and bearings.

Six gears were designed to transmit torque and reduce speed. A four-gear configuration was initially considered but required excessively strong intermediate shaft gears to handle high fatigue stress. Numerical iteration demonstrated that a six-gear configuration with two auxiliary shafts reduced weight more effectively. A Python-based optimization program then identified the optimal gear configuration to reduce weight as 21:59:19:45 for gears 1, 2, 3, and 4 respectively, with diametral pitches of 10 for Gearset 1, and 8 for Gearset 2. The smaller diametral pitch for Gearset 2 was set to increase face width and reduce the stress on the output gears. The critical safety factor of 1.675 aligns with the predefined range, with the smallest safety factor being 1.67 for the third gear, ensuring a controlled failure progression and helping avoid a catastrophic failure. This safety factor was achieved using nitrided AISI 4340 steel for gears 3 and 4, and Ti-6Al-4V for gears 1 and 2.

The gearbox includes four shafts – two auxiliary, one input, and one propeller shaft – designed to transmit torque through the keys to the gears and support gears and bearings. All shafts are made from AISI 1045 cold-rolled steel, with diameters and geometries optimized based on their respective locations and stress distributions along them. The design ensures compatibility with gear dimensions while minimizing weight. Stress concentrations at keyways, shoulder fillets, and maximum stress location were analyzed, resulting in safety factors of at least 1.75 everywhere along the shafts, indicating safe and reliable designs.

Keys transmit torque between gears and shafts. In this design, standard sizes of squared cross-section keys were selected based on shaft diameters, with lengths adjusted to achieve the desired safety factor. To ensure keys fail first as intended in the failure hierarchy of our design, AISI 1020 cold-rolled steel, which has a lower yield stress, was selected. The length of the keys was then adjusted to achieve the required safety factors of 1.5.

The gearbox contains six bearings selected based on load, speed, and lifespan requirements. Ball bearings from the SKF catalogue were selected for shafts 1, 2, and 3 due to their moderate radial loads and speeds. The output shaft uses a higher capacity ball bearing combined with a tapered roller bearing at location 6 to support the axial and radial loads caused by the propeller. The larger contact area of the tapered

roller bearing ensures that the load is being distributed efficiently. The bearing life for all bearings surpass the required life at all locations, ensuring a reliable selection.

Overall, the design meets all the requirements, with shafts and gears fitting within the provided gearbox limit dimensions. The total gear ratio is 6.654, which yields an output velocity of 826.57 RPM, and the gearbox is designed for worst-case conditions, assuming maximum input power across all loading cycles. This ensures a safe and reliable design, and a lifespan exceeding the required 2000 hours. The final design was optimized so that the total weight of the gearbox is 15.84 kilograms.

Future improvements could optimize gears and shafts for enhanced performance, efficiency and reliability. Lightweight materials like high-strength alloys or composites could reduce gear weight without compromising durability, while refined tooth profiles and surface treatments such as carburizing or DLC coatings could improve load distribution and wear resistance. Hollow shafts or lightweight alloys could reduce weight while maintaining strength, and integrated sensors could enable real-time torque and stress monitoring for predictive maintenance. Upgrading to high-precision or ceramic bearings could further minimize friction and enhance efficiency. Advanced thermal management, such as cooling fins or optimized lubrication, could improve heat dissipation and extend component lifespan.

In conclusion, this project successfully applied AGMA standards and industry guidelines to design a robust, efficient gearbox, prioritizing reliability, lightweight, and predictable failure modes. Moreover, this project highlighted the importance of numerical methods in optimizing mechanical designs, using iterative calculations to minimize gearbox weight while ensuring structural integrity and operational safety.

The success of this project can be attributed to the meticulous application of the standardized design processes and the integration of computational tools. Ultimately, reliability, light-weight characteristics and predictable failure behavior of the gearbox are the direct result of the team's efforts to precision, innovation and standardization in mechanical design.

6. References

[1] https://ntrs.nasa.gov/api/citations/20150003482/downloads/20150003482.pdf

[2] R. L. Norton, *Machine design: An integrated approach*, 6th ed. Pearson, 2021.

[3] MatWeb, "AISI 1045 Steel, cold drawn," Nov. 2, 2024. [Online]. Available: https://www.matweb.com/search/datasheet.aspx?matguid=cbe4fd0a73cf4690853935f52d910784&ckck=1.

[4] MatWeb, "AISI 1020 Steel, cold rolled," Nov. 2, 2024. [Online]. Available: https://www.matweb.com/search/datasheet.aspx?matguid=10b74ebc27344380ab16b1b69f1cffbb&ckck=1.

[5] SKF, "Rolling bearings," *SKF*, Nov. 28, 2024. [Online]. Available: https://www.skf.com/us/products/rolling-bearings.

[6] SKF, "Speed limitations," *SKF*, Nov. 28, 2024. [Online]. Available: https://www.skf.com/us/products/rolling-bearings/principles-of-rolling-bearing-selection/bearing-selection-process/operating-temperature-and-speed/speed-limitations.

[7] MatWeb, "Gray Cast Iron, ASTM A 48 Class 40," Nov. 2, 2024. [Online]. Available: https://www.matweb.com/search/DataSheet.aspx?MatGUID=ec56a89f37f74e2f867a64b0f87f1e9d.

[8] MatWeb, "Titanium Ti-6Al-4V (Grade 5), Annealed," Nov. 12, 2024. [Online]. Available: https://www.matweb.com/search/DataSheet.aspx?MatGUID=a0655d261898456b958e5f825ae85390&ckck=1.

[9] "Understanding Precision CNC Machining Tolerances," Staub Inc., [Online]. Available: https://staubinc.com/news/understanding-precision-cnc-machining-tolerances/. [Accessed: 01-Dec-2024].

7. Appendices

Appendix A. Design Requirements and Important Specifications

Configuration and Performance			
Operation	**Duration (min)**	**Electric power to Motor Driver (HP)**	**RPM**
Take-Off	10	60	5500
Slow Climb	15	10	2500
Steep Climb	15	15	2570
Descent Glide	30	2.5	2000
Horizontal Flight	120	5	2550
Gearbox Specifications			
Gear Ratio	TBD		
Total weight (optimal)	5.5 kg		
Endurance/life	2,000 hrs		
Temperature range	-40 to +40 deg C		
Size limitations for integration	30 cm x 45 cm x 45 cm (x,y & z) x = flight direction y = wing axis z = vertical axis		
Propeller Specifications			
Weight	100 kg		
Max RPM (Take-off)	835		
Location of center of gravity	10 cm from shaft support bearing (x-coordinate)		

Appendix B. Numerical optimization method for gear teeth number combination

```
import math
import scipy.optimize
gear_ratios = []
current_value = 1.8
while current_value <= 3.8:
    gear_ratios.append(round(current_value, 1))
    current_value += 0.1

total_ratio = 6.6  # Total gear ratio
pd_12 = 12
pd_34 = 8  # Variable diametral pitch for gear 1 2 and gear 3 4
min_teeth = 18  # Minimum number of teeth (avoid interference)

# Gear teeth combination validity
def is_valid_combination(N1, N2, N3, N4):
    """Minimum number of teeth criterion"""
    if N1 < min_teeth or N2 < min_teeth or N3 < min_teeth or N4 < min_teeth:
        return False
    return True

def geometry_constraints(N1, N2, N3, N4):
    """Parallel axis criterion"""
    if N1 > N2 or N3 > N4:
        return False
    if 4 * (N1 + N2) != 5 * (N3 + N4):   # For variable diametral pitch: 3(N1+N2) = 2(N3+N4)
        return False
    return True

def y_span_constraint(N1, N2, N3, N4):
    """The y-span should be smaller than 45 cm (17.7165354 inch)"""
    y_span = 0.5 * ((N2 / pd_12) + (N4 / pd_34) + (N2 / pd_12) + (N1 / pd_12))
    if y_span > 17.7165354:
        return False
    return True

# Iteration starts
valid_results = []
for ratio1 in gear_ratios:
    ratio2 = total_ratio / ratio1  # Calculate gear ratio 2


    # Teeth number relations
    for N2 in range(min_teeth, 101):  # Iteration maximum value 100
        N1 = round(N2 / ratio1)
        N3 = int((4 * (1 + 1 / ratio1) * N1) / (5 * (1 + 1 / ratio2)))
        N4 = round(N3 / ratio2)

        if not is_valid_combination(N1, N2, N3, N4):
            continue
        if not geometry_constraints(N1, N2, N3, N4):
            continue
        if not y_span_constraint(N1, N2, N3, N4):
            continue

        # Check total gear ratio > 6.6
        actual_ratio = (N2 / N1) * (N4 / N3)
        if actual_ratio >= total_ratio:
            max_y_span = round(0.5 * ((N2 / pd_12) + (N4 / pd_34) + (N2 / pd_12) + (N1 / pd_12))) * 2.54
            unit_conversion = 16.387064   # in^3 to cm^3
            gear_13_material = 7.85   # g/cm^3
            gear_24_material = 7.15   # g/cm^3
            gear_1_mass = ((0.5 * (N1 / pd_12)) ** 2 * math.pi * (12 / pd_12)) * unit_conversion * gear_13_material
            gear_2_mass = ((0.5 * (N2 / pd_12)) ** 2 * math.pi * (12 / pd_12)) * unit_conversion * gear_24_material
            gear_3_mass = ((0.5 * (N3 / pd_12)) ** 2 * math.pi * (12 / pd_34)) * unit_conversion * gear_13_material
            gear_4_mass = ((0.5 * (N4 / pd_12)) ** 2 * math.pi * (12 / pd_34)) * unit_conversion * gear_24_material
            total_mass = gear_1_mass + gear_2_mass + gear_3_mass + gear_4_mass
            valid_results.append((N1, N2, N3, N4, max_y_span, actual_ratio, total_mass))

# Results
if valid_results:
    print("Valid gear teeth combination:")
    for result in valid_results:
        print(f"N1={result[0]}, N2={result[1]}, N3={result[2]}, N4={result[3]}, max y span={result[4]} cm, total gear
ratio={result[5]:.2f}, total gear mass={result[6]} g")
else:
    print("No valid gear teeth combination")
```

Appendix C. Useful Graphs, Tables, and Figures from the Textbook

Table 12-9 AGMA Bending Geometry Factor J for 20°, Full-Depth Teeth with HPSTC Loading

Gear teeth	Pinion teeth: 12 P	12 G	14 P	14 G	17 P	17 G	21 P	21 G	26 P	26 G	35 P	35 G	55 P	55 G	135 P	135 G
12	U	U														
14	U	U	U	U												
17	U	U	U	U	U	U										
21	U	U	U	U	U	U	0.33	0.33								
26	U	U	U	U	U	U	0.33	0.35	0.35	0.35						
35	U	U	U	U	U	U	0.34	0.37	0.36	0.38	0.39	0.39				
55	U	U	U	U	U	U	0.34	0.40	0.37	0.41	0.40	0.42	0.43	0.43		
135	U	U	U	U	U	U	0.35	0.43	0.38	0.44	0.41	0.45	0.45	0.47	0.49	0.49

Figure C.1: AGMA Bending Geometry Factor J for 20°, Full-Depth Teeth with HPSTC Loading

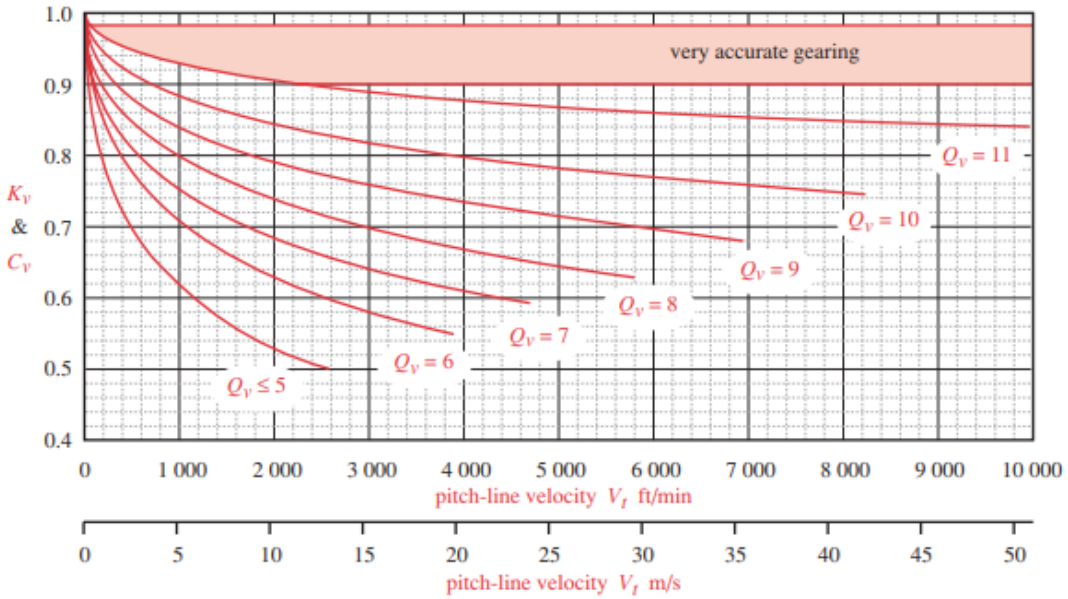

Figure C.2: Correlation between dynamic factors and pitch-line velocity

Table 12-6

Recommended AGMA Gear Quality Numbers for Various Applications

Application	Q_v
Cement mixer drum drive	3–5
Cement kiln	5–6
Steel mill drives	5–6
Corn picker	5–7
Cranes	5–7
Punch press	5–7
Mining conveyor	5–7
Paper-box making machine	6–8
Gas meter mechanism	7–9
Small power drill	7–9
Clothes washing machine	8–10
Printing press	9–11
Computing mechanism	10–11
Automotive transmission	10–11
Radar antenna drive	10–12
Marine propulsion drive	10–12
Aircraft engine drive	10–13
Gyroscope	12–14

Figure C.3: Recommended AGMA Gear Quality Numbers for Various Applications

Table 12-16

Load Distribution Factors K_m

Face Width in	(mm)	K_m
<2	(50)	1.6
6	(150)	1.7
9	(250)	1.8
≥20	(500)	2.0

Figure C.4: Load Distribution Factors K_m

Table 12-17 Application Factors K_a

Driving Machine	Driven Machine: Uniform	Moderate Shock	Heavy Shock
Uniform (Electric motor, turbine)	1.00	1.25	1.75 or higher
Light Shock (Multicylinder engine)	1.25	1.50	2.00 or higher
Medium Shock (Single-cylinder engine)	1.50	1.75	2.25 or higher

Figure C.5: Application Factors K_a

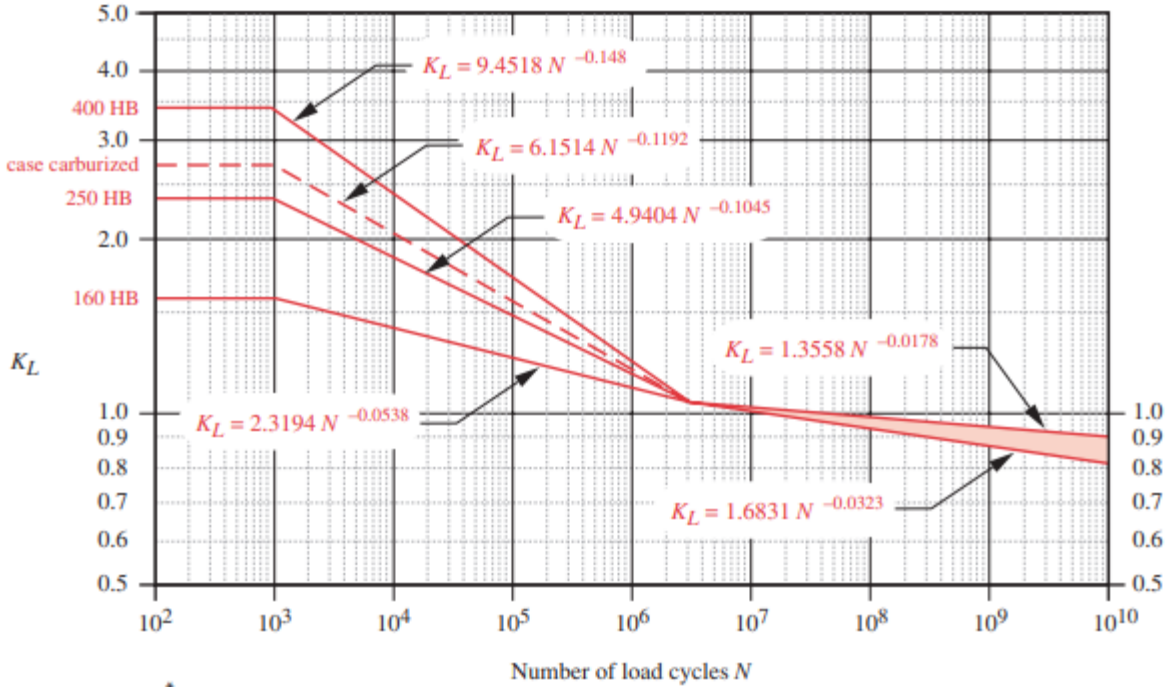

Figure C.6: AGMA Bending Strength Life Factor K_L

Table 12-19
AGMA Factor K_R

Reliability %	K_R
90	0.85
99	1.00
99.9	1.25
99.99	1.50

Figure C.7: AGMA Factor K_R

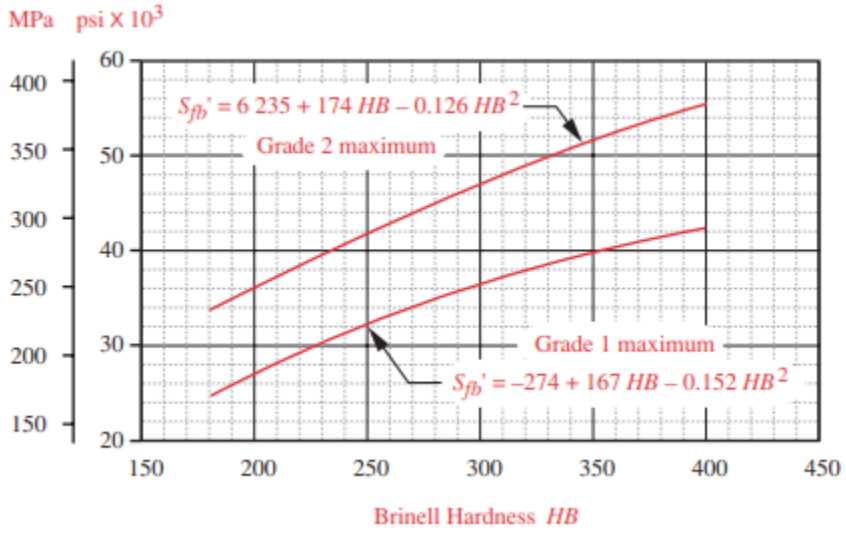

Figure C.8: AGAM Bending-Fatigue Strengths S'_{fb} for Steels

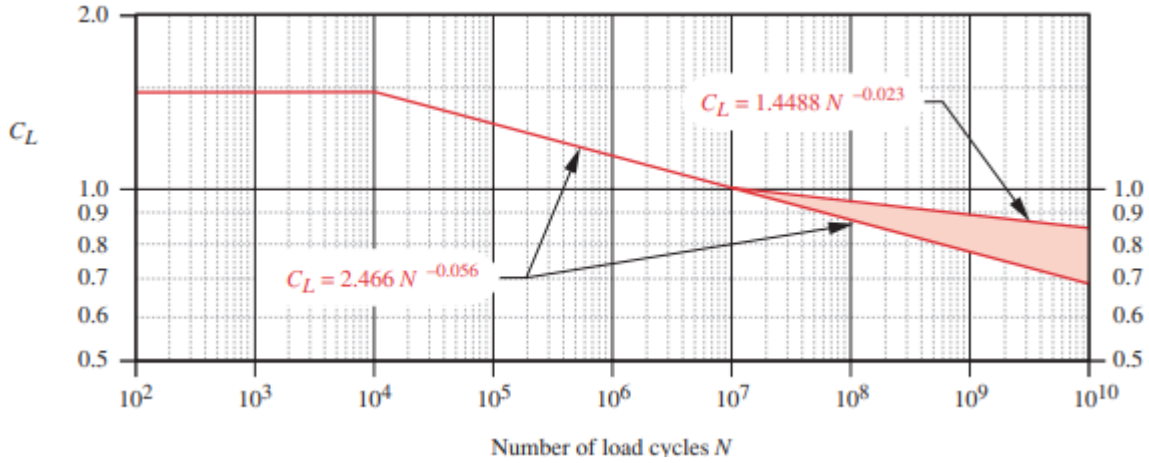

Figure C.9: AGAM Surface-Fatigue Strength Life Factor C_L

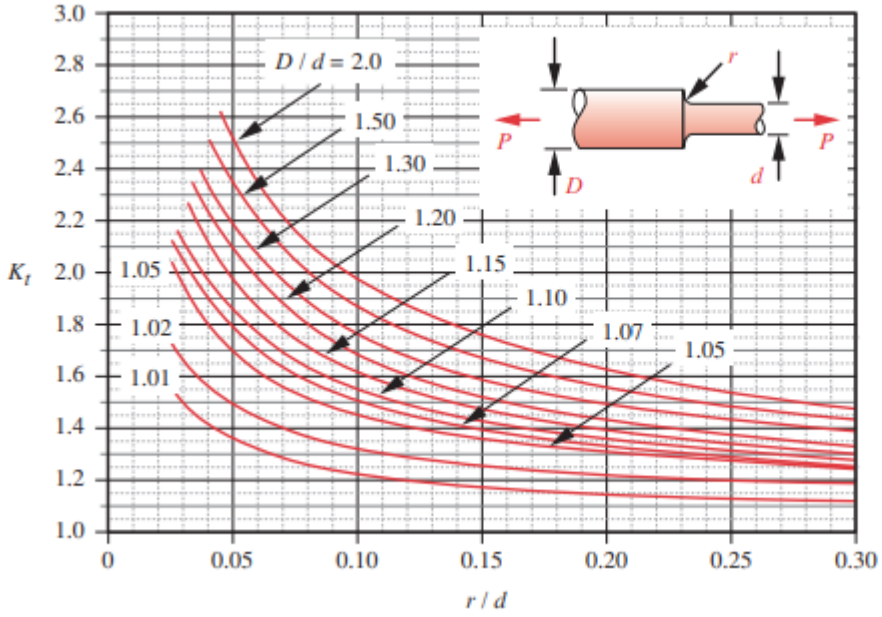

$$K_t \equiv A\left(\frac{r}{d}\right)^b$$

where :

D/d	A	b
2.00	1.014 70	–0.300 35
1.50	0.999 57	–0.282 21
1.30	0.996 82	–0.257 51
1.20	0.962 72	–0.255 27
1.15	0.980 84	–0.224 85
1.10	0.984 50	–0.208 18
1.07	0.984 98	–0.195 48
1.05	1.004 80	–0.170 76
1.02	1.012 20	–0.124 74
1.01	0.984 13	–0.104 74

Figure C.10: Stress-Concentration Factor K_t for a Circular Shaft with a Shoulder Fillet in Axial Tension

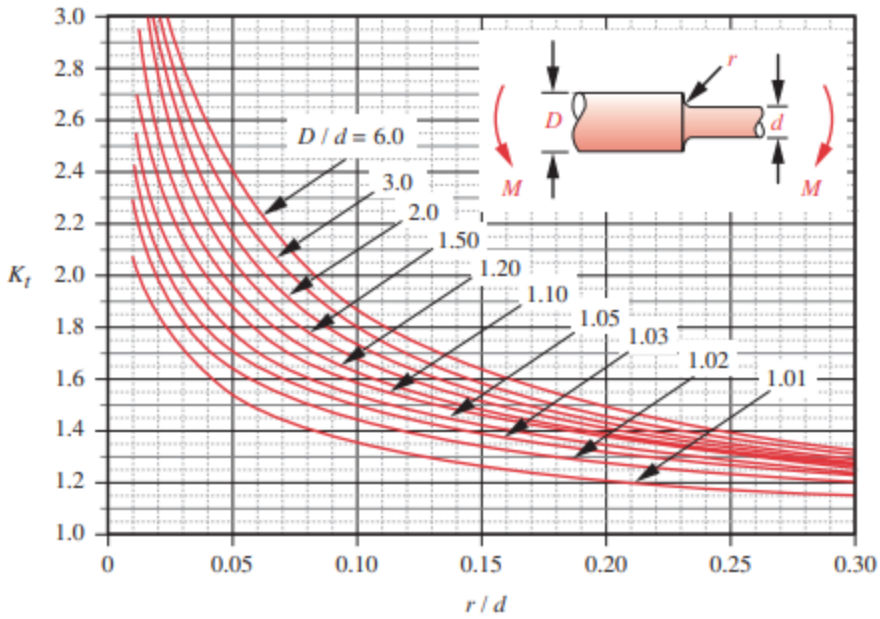

$$K_t \equiv A\left(\frac{r}{d}\right)^b$$

where :

D / d	A	b
6.00	0.878 68	–0.332 43
3.00	0.893 34	–0.308 60
2.00	0.908 79	–0.285 98
1.50	0.938 36	–0.257 59
1.20	0.970 98	–0.217 96
1.10	0.951 20	–0.237 57
1.07	0.975 27	–0.209 58
1.05	0.981 37	–0.196 53
1.03	0.980 61	–0.183 81
1.02	0.960 48	–0.177 11
1.01	0.919 38	–0.170 32

Figure C.11: Stress-Concentration Factor K_t for a Circular Shaft with a Shoulder Fillet in Bending

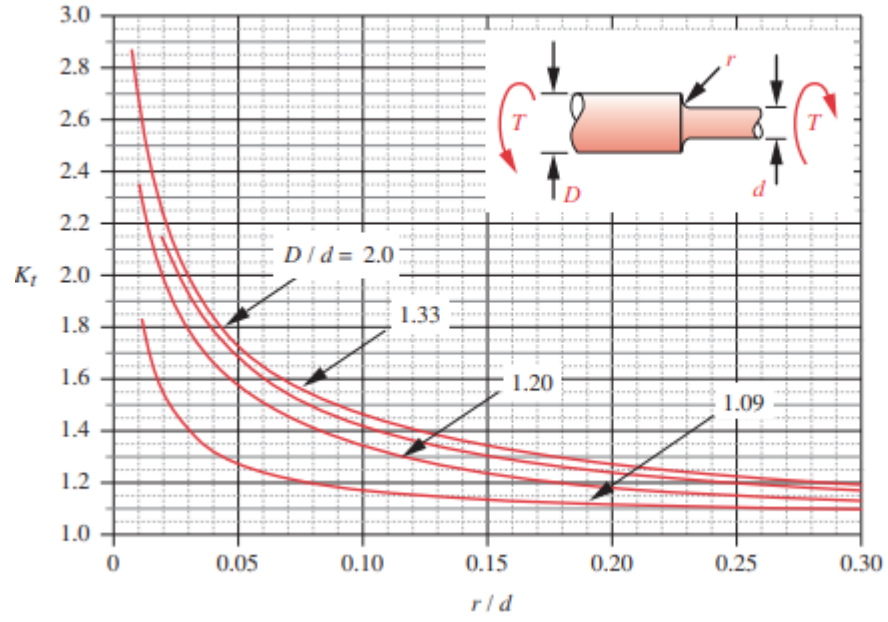

$$K_t \equiv A\left(\frac{r}{d}\right)^b$$

where :

D / d	A	b
2.00	0.863 31	–0.238 65
1.33	0.848 97	–0.231 61
1.20	0.834 25	–0.216 49
1.09	0.903 37	–0.126 92

Figure C.12: Stress-Concentration Factor K_{ts} for a Circular Shaft with a Shoulder Fillet in Torsion

Table 6-6
Neuber's Constant for Steels

S_{ut} (ksi)	$\sqrt{a}$ ($in^{0.5}$)
50	0.130
55	0.118
60	0.108
70	0.093
80	0.080
90	0.070
100	0.062
110	0.055
120	0.049
130	0.044
140	0.039
160	0.031
180	0.024
200	0.018
220	0.013
240	0.009

Figure C.13: Neuber's Constant for Steels with Different Ultimate Tensile Strength

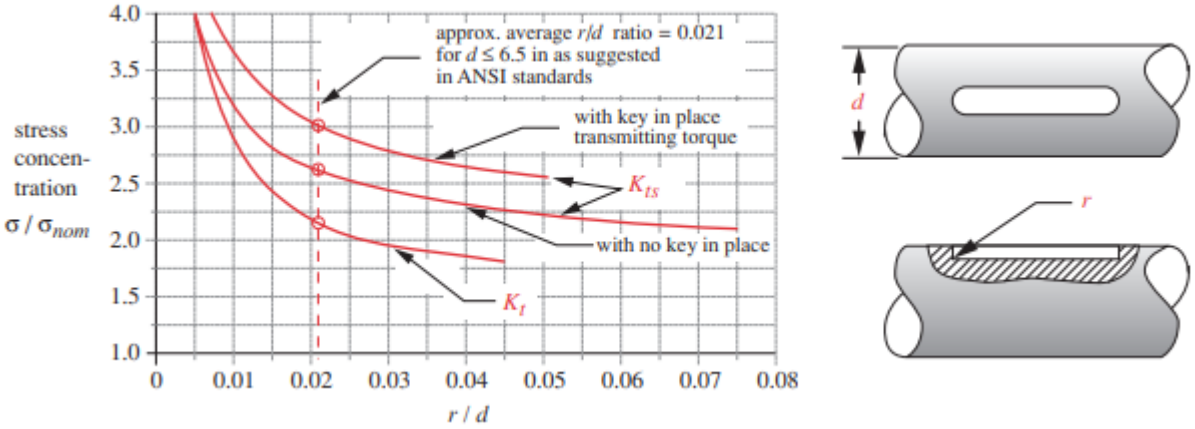

Figure C.14: Keyway Concentration Factors for Different r/d Ratios

Table 6-3 **Coefficients for Surface-Factor Equation 6.7e**
Source: Shigley and Mischke, *Mechanical Engineering Design*, 5th ed., McGraw-Hill, New York, 1989, p. 283 with permission

	For S_{ut} in MPa use		For S_{ut} in kpsi (not psi) use	
Surface Finish	A	b	A	b
Ground	1.58	–0.085	1.34	–0.085
Machined or cold-rolled	4.51	–0.265	2.7	–0.265
Hot-rolled	57.7	–0.718	14.4	–0.718
As-forged	272	–0.995	39.9	–0.995

Figure C.15: Coefficient for Surface Factor Equations

Table 6-4
Reliability Factors
for $S_d = 0.08\ \mu$

Reliability %	C_{reliab}
50	1.000
90	0.897
95	0.868
99	0.814
99.9	0.753
99.99	0.702
99.999	0.659
99.9999	0.620

Figure C.16: Reliability Correction Factors for Different Reliability Factors

Table 10-2 Standard Key and Setscrew Sizes for US and Metric Sized Shafts

Shaft Diameter (in)	Nominal Key Width (in)	Setscrew Dia. (in)	Shaft Diameter (mm)	Key Width x Height (mm)
$0.312 < d \leq 0.437$	0.093	#10	$8 < d \leq 10$	3 x 3
$0.437 < d \leq 0.562$	0.125	#10	$10 < d \leq 12$	4 x 4
$0.562 < d \leq 0.875$	0.187	0.250	$12 < d \leq 17$	5 x 5
$0.875 < d \leq 1.250$	0.250	0.312	$17 < d \leq 22$	6 x 6
$1.250 < d \leq 1.375$	0.312	0.375	$22 < d \leq 30$	8 x 7
$1.375 < d \leq 1.750$	0.375	0.375	$30 < d \leq 38$	10 x 8
$1.750 < d \leq 2.250$	0.500	0.500	$38 < d \leq 44$	12 x 8
$2.250 < d \leq 2.750$	0.625	0.500	$44 < d \leq 50$	14 x 9
$2.750 < d \leq 3.250$	0.750	0.625	$50 < d \leq 58$	16 x 10
$3.250 < d \leq 3.750$	0.875	0.750	$58 < d \leq 65$	18 x 11
$3.750 < d \leq 4.500$	1.000	0.750	$65 < d \leq 75$	20 x 12
$4.500 < d \leq 5.500$	1.250	0.875	$75 < d \leq 85$	22 x 14
$5.500 < d \leq 6.500$	1.500	1.000	$85 < d \leq 95$	25 x 14

Figure C.17: Standard Key and Setscrew Sizes for US and Metric Sized Shafts

Factors V, X, and Y for Radial Bearings

Bearing Type			In Relation to the Load the Inner Ring is		Single Row Bearings 1)		Double Row Bearings 2)				e
			Rotating	Stationary	$\frac{F_a}{VF_r} > e$		$\frac{F_a}{VF_r} \leq e$		$\frac{F_a}{VF_r} > e$		
			V	V	X	Y	X	Y	X	Y	
3) Radial Contact Groove Ball Bearings	4) $\frac{F_a}{C_0}$	5) $\frac{F_a}{i Z D_w^2}$									
	0.014	25	1	1.2	0.56	2.30	1	0	0.56	2.30	0.19
	0.028	50				1.99				1.99	0.22
	0.056	100				1.71				1.71	0.26
	0.084	150				1.55				1.55	0.28
	0.11	200				1.45				1.45	0.30
	0.17	300				1.31				1.31	0.34
	0.28	500				1.15				1.15	0.38
	0.42	750				1.04				1.04	0.42
	0.56	1000				1.00				1.00	0.44
20°			1	1.2	0.43	1.00	1	1.09	0.70	1.63	0.57
25°					0.41	0.87		0.92	0.67	1.44	0.68
30°					0.39	0.76		0.78	0.63	1.24	0.80
35°					0.37	0.66		0.66	0.60	1.07	0.95
40°					0.35	0.57		0.55	0.57	0.93	1.14
Self-Aligning Ball Bearings			1	1	0.40	0.4 cot α	1	0.42 cot α	0.65	0.65 cot α	1.5 tan α
Self-Aligning and Tapered Roller Bearings			1	1.2	0.40	0.4 cot α	1	0.45 cot α	0.67	0.67 cot α	1.5 tan α

1) For single row bearings, when $\frac{F_a}{VF_r} \leq e$ use $X = 1$ and $Y = 0$.

For two single row angular contact ball or roller bearings mounted "face-to-face" or "back-to-back" the values of X and Y which apply to double row bearings. For two or more single row bearings mounted "in tandem" use the values of X and Y which apply to single row bearings.

2) Double row bearings are presumed to be symmetrical.

3) Permissible maximum value of $\frac{F_a}{C_0}$ depends on the bearing design.

4) C_0 is the basic static load rating.

5) Units are pounds and inches.

Values of X, Y and e for a load or contact angle other than shown in the table are obtained by linear interpolation.

Figure C.18: Factors V, X, and Y for Radial Bearings

Appendix D. Gear Sample Calculations

D.1 Maximum Gear Ratio for The Double Reduction Gearbox

Total torque ratio:

$$r_{total,torque} = \frac{\omega_{out}}{\omega_{in}} = \frac{5500\ RPM}{835\ RPM} = 6.5868$$

Total velocity ratio:

$$r_{total,velocity} = \frac{\omega_{in}}{\omega_{out}} = \frac{835\ RPM}{5500\ RPM} = 0.151818$$

The maximum total gear ratio is determined by the total torque ratio since it is greater than 1.

D.2 Minimum number of teeth

The minimal number of teeth on a gear to avoid undercutting and interference can be determined using the following method:

$$N_{min} = \frac{2}{sin^2\emptyset}$$

The symbol $\emptyset$ denotes the pressure angle of the gear. In this design, the pressure angle is set to be 20°.

$$N_{min} = \frac{2}{sin^2\emptyset} = \frac{2}{sin^2 20^{\circ}} = 17.097 \approx 18$$

The calculation result is slightly higher than 17. The value is rounded up to the next integer to avoid gear interference.

D.3 Compound Gear Teeth Number

From the fundamental gear law, we can obtain two equations for gear sets 1 and 2:

Gear set 1:

$$r_1 = \frac{N_2}{N_1} \quad (1)$$

Gear set 2:

$$r_2 = \frac{N_4}{N_3} \quad (2)$$

Since the input shaft and the output shaft need to be coaxial, the sum of radius of Gear 1 and Gear 2 should be equal to the sum of radius of Gear 3 and Gear 4. Mathematically, the geometric relationship is shown below.

Geometry constraint: $\frac{N_1}{Pd_1} + \frac{N_2}{Pd_1} = \frac{N_3}{Pd_2} + \frac{N_4}{Pd_2} \quad \rightarrow \quad \frac{N_1+N_2}{10} = \frac{N_3+N_4}{8}$ (3)

In this design, the initial iterative variable is set to be Gear 2. Thus, the teeth number of Gear 2 can be treated as a known variable. Rearrange equation (1) and (2), the values of N_1 and N_3 can be expressed as:

Gear 1 number of teeth: $N_1 = \frac{N_2}{r_1}$ (4)

Gear 2 number of teeth: $N_3 = \frac{N_4}{r_2}$ (5)

Now, combine equations (3), (4) and (5). The three equations form a system with three unknowns. Plug in $N_2 = 59$ into the system of equations:

$$4\left(1 + \frac{1}{r_1}\right)(59) = 5\left(1 + \frac{1}{r_2}\right)N_4$$

All unknown variables can be solved:

$$N_4 = 45$$

$$N_3 = \frac{N_4}{r_2} = \frac{45}{2.36842} = 19$$

$$N_1 = \frac{N_2}{r_1} = \frac{59}{2.80952} = 21$$

D.4: Individual Gear Ratio for Gear Set 1 and Gear Set 2

Gear ratio for gear set 1:

$$r_1 = \frac{N_2}{N_1} = \frac{59}{21} = 2.80952$$

Gear ratio for gear set 2:

$$r_2 = \frac{N_3}{N_4} = \frac{45}{19} = 2.36842$$

Total gear ratio: $r_{total} = r_1 \times r_2 = 2.80952 \times 2.36842 = 6.654$

By comparing the maximum actual total gear ratio and the maximum required total gear ratio, we can conclude that the gear teeth combination used in this design satisfies the speed reduction requirement.

D.5 Gear Geometry Parameters

The calculations for the main geometry parameters of gear 1 are shown below; these parameters were computed in the same manner for the other gears.

- Gear 1 pitch diameter:

$$d_p = \frac{N_1}{Pd_1} = \frac{21}{10} = 2.1\ in$$

- Gear 1 pitch circle:

$$P_c = \frac{\pi \times d_p}{N_1} = \frac{\pi \times 2.1}{21} = 0.31415\ in/teeth$$

- Gear 1 addendum:

$$a = \frac{1}{P_d} = \frac{1}{10} = 0.1\ in/teeth$$

- Gear 1 dedendum:

$$b = \frac{1.25}{P_d} = \frac{1.25}{10} = 0.125\ in/teeth$$

- Gear 1 face width:

$$F = \frac{13}{P_d} = \frac{13}{10} = 1.3\ in$$

D.6 Torque Analysis

The following torque analysis is presented in the gear section. Though, the torques computed apply also to the shafts and bearings.

Maximum input torque:

$$T_1 = \frac{P}{\omega} = \frac{(60\ hp) \times (6600\ \frac{in \cdot lb}{s \cdot hp})}{5500\ RPM \cdot (2\pi/60) \cdot (\frac{rad}{s \cdot RPM})} = 687.55\ lb \cdot in = 57.29\ lb \cdot ft$$

Maximum input speed on the auxiliary shaft:

$$\omega_2 = \frac{\omega_1}{r_1} = \frac{5500\ RPM}{2.80952} = 1957.63\ RPM$$

Maximum torque in shaft 2 and 3:

$$T_2 = \frac{P}{\omega_2} = \frac{(60\ hp) \times (6600\ \frac{in \cdot lb}{s \cdot hp})}{1957.63\ RPM \cdot (2\pi/60) \cdot (\frac{rad}{s \cdot RPM})} = 1931.68\ lb \cdot in = 160.97\ lb \cdot ft$$

Maximum rotational speed on the output shaft:

$$\omega_3 = \frac{\omega_1}{r_1 \cdot r_2} = \frac{5500\ RPM}{2.80952 \cdot 2.36842} = 826.555\ RPM$$

Maximum output torque:

$$T_3 = T_{input} \cdot r_{total} = 57.29\ lb \cdot ft \times 6.654 = 381.2\ lb \cdot ft$$

Once the torques have been computed, the tangential component of the load transmitted to a gear can be found as presented below. Note that this calculation is for the first pinion gear, though the procedure remains the same for the second gear set.

$$W_t = \frac{T_1}{d_p/_2} = \frac{2(687.55)}{2.1} = 654.81\ lbf$$

Note that since pinion 1 transmits a load to two gears: gear 2 and 2', then the load transmitted is half of the above value:

$$W_t = 327.40\ lbf$$

D.7 Y-Span and Z-Span of The Reduction Gearbox

The determination of the Z-span of the reduction gearbox is relatively simple. It is governed by the largest gear in the gearbox design. In this case, the largest gear diameter is 5.9 inches (15 cm). Hence, the Z-span of the gearbox design is 15 cm, within the design envelop on the Z-axis.

The Y-span of the reduction gearbox is determined by the largest sum of the gear set's diameters.

Sum of gear set 1 diameter: $\sum d_i = d_{gear\ 1} + 2 \times d_{gear\ 2} = 13.9\ in = 35.306\ cm$

Sum of gear set 2 diameter: $\sum d_i = d_{gear\ 4} + 2 \times d_{gear\ 3} = 8.3\ in = 21.082\ cm$

The largest sum of diameters occurs at gear set 1. Therefore, the Y-span of the gearbox design is 35.3 cm.

D.8 Gear Life and Cycle Analysis

To simplify the calculation, the total time for one flight mission is approximated to 3 hours instead of 3 hours and 10 minutes. To design a gearbox with 2000 hours of life, the total number of missions in the gear lifetime is calculated:

$$N_{mission} = \frac{Endurance}{operation\ hour\ per\ flight} = \frac{2000\ hr}{3\ hr} = 666.67 \approx 667$$

Given the time span of each flight stage in one mission, the total working time in each stage can be determined. This is the critical step to accurately determine the number of loading-unloading cycles in gears lifetime.

- Total operation time for take-off:
$$T_{take\ off} = mission\ \# \times take\ off\ time = 6670\ min$$
- Total operation time for slow climb:
$$T_{slow\ climb} = mission\ \# \times slow\ climb\ time = 6670\ min$$
- Total operation time for steep climb:
$$T_{steep\ climb} = mission\ \# \times steep\ climb\ time = 6670\ min$$
- Total operation time for horizontal flight:
$$T_{horizontal} = mission\ \# \times cruise\ time = 80040\ min$$
- Total operation time for descent glide:
$$T_{descent} = mission\ \# \times descent\ glide\ time = 20010\ min$$

Table D.8.1: Gear Life Span Analysis Under Different Working Conditions

Operations	Duration per flight	Motor input power	Rotational speed	Life-time duration
Take-off	10 min	60 HP	5500 RPM	6670 min
Slow climb	10 min	10 Hp	2500 RPM	6670 min
Steep climb	10 min	15 HP	2570 RPM	6670 min
Cruise	120 min	5 HP	2550 RPM	80040 min
Descent glide	30 min	2.5 HP	2000 RPM	20010 min

Take Gear 1 as an example. Due to the special gear configuration, Gear 1 will experience two loading and unloading cycles in one revolution. This is because the gear meshes with two other gears (Gear 2 and Gear 2'). Hence, in the computation of cycle number for Gear 1 (also the output Gear 4), one needs to double the cycle number. The total number of cycles for Gear 1 can be calculated as:

- Cycle number in take-off:
$$N = 2 \times 5500\ RPM \times 6670\ \text{min} = 73370000\ cycles$$
- Cycle number in slow climb:
$$N = 2 \times 2500\ RPM \times 6670\ \text{min} = 33350000\ cycles$$
- Cycle number in steep climb:
$$N = 2 \times 2570\ RPM \times 6670\ \text{min} = 34283800\ cycles$$
- Cycle number in horizontal flight:
$$N = 2 \times 2550\ RPM \times 80040\ \text{min} = 80040000\ cycles$$
- Cycle number in descent glide:
$$N = 2 \times 2000\ RPM \times 20010\ \text{min} = 40020000\ cycles$$
- Total number of cycles in Gear 1 lifetime:
$$N_{total} = 261063800\ cycles$$

D.9 Gears' Material Selection

Table D.9.1: Materials Properties of Different Analyzed Materials [2,5,6]

Material	Density [g/cm^3]	Elastic Modulus [*kpsi*]	Fatigue Strength [*psi*]	Hardness [*HB*]
Nitrided AISI 4340 (Nitrided)	7.85	29000	50800	552
Cast iron	7.15	22000	18600	235
Titanium alloy (Ti-6Al-4V)	4.5	16510	87000	336

D.10 Stress and Load Analysis for Gear Set 1

Gear ratio: $m_G = \frac{59}{21} = 2.80952381$

Life cycle of pinion and gears: $N_p = 261063800\ cycles$, $N_g = 111984778\ cycles$

Torque on pinion: $T_p = \frac{P}{\omega_p} = \frac{60*6600}{5500*\left(\frac{2\pi}{60}\right)} = 687.5493542\ lb*in$

Pitch diameter of pinion and gears: $d_p = \frac{N_1}{P_d} = \frac{21}{10} = 2.1\ in$, $d_g = \frac{N_2}{P_d} = \frac{59}{10} = 5.9\ in$

Transmitted load: $W_t = \frac{\frac{T_p}{d_p}}{2} = \frac{\frac{687.5493542}{2.1}}{2} = 327.4044544\ lb$

Face width: $F = \frac{13}{P_d} = \frac{13}{10} = 1.3\ in$

Tangential velocity of pinion: $V_t = d_p * \omega_p * \frac{2\pi}{2*12} = 2.1 * 5500 * \frac{2\pi}{2*12} = 3023.782929\ \frac{ft}{min}$

Correction factors of bending stress: $K_a = 1$, $K_m = 1.6$, $K_v = 0.89$, $K_s = 1.25$, $K_I = 1$, $K_B = 1$ $J_p = 0.3404$, $J_g = 0.4015$

Bending stress of pinion: $\sigma_{b,p} = \frac{W_t p_d}{F J_p}\frac{K_a K_m}{K_v} K_S K_B K_I = 327.404 * 10 * 1.6 * \frac{1.25}{1.3*0.3404*0.89} = 13300.91922\ psi$

Bending stress of each gear: $\sigma_{b,g} = \frac{W_t p_d}{F J_g}\frac{K_a K_m}{K_v} K_S K_B K_I = 327.404 * 10 * 1.6 * \frac{1.25}{1.3*0.4015*0.89} = 11276.79428\ psi$

Bending-fatigue strength before correction: $S_{fb'} = 102HB + 16400 = 102 * 336 + 16400 = 50672\ psi$

Correction factors of bending-fatigue strength: $K_{L,p} = 1.6831\left(N_p\right)^{-0.0323} = 0.900013457$, $K_{L,g} = 1.6831\left(N_g\right)^{-0.0323} = 0.924958152$, $K_t = 0.9097$, $K_r = 1$

Bending-fatigue strength of pinion: $S_{fb,p} = \frac{K_{L,p}}{K_T K_R} S_{fb'} = 0.9 * \frac{50672}{0.9097} = 50132.44134\ psi$

Bending-fatigue strength of each gear: $S_{fb,g} = \frac{K_{L,g}}{K_T K_R} S_{fb'} = 0.925 * \frac{50672}{0.9097} = 51521.90777\ psi$

Bending safety factor of pinion: $N_{b,p} = \frac{S_{fb,p}}{\sigma_{b,p}} = \frac{50132.44134}{13300.91922} = 3.769095992$

Bending safety factor of each gear: $N_{b,g} = \frac{S_{fb,g}}{\sigma_{b,g}} = \frac{50132.44134}{11276.79428} = 4.568843457$

Correction factors of surface stress: $C_a = 1$, $C_m = K_m = 1.6$, $C_v = K_v = 0.89$, $C_f = 1$, $C_s = K_s = 1$

$$C_p = \sqrt{\frac{1}{\pi\left[\left(\frac{1-v_p^2}{E_p}\right) + \left(\frac{1-v_g^2}{E_g}\right)\right]}} = \sqrt{\frac{1}{\pi\left[\left(\frac{1-0.342^2}{16510*1000}\right) + \left(\frac{1-0.342^2}{16510*1000}\right)\right]}} = 1724.498$$

$$\rho_1 = \sqrt{\left(r_p + \frac{1}{p_d}\right)^2 - (r_p cos\varphi)^2} - \frac{\pi}{P_d cos\varphi} = \sqrt{\left(\frac{2.1}{2} + \frac{1}{10}\right)^2 - (\frac{2.1}{2} * cos20^\circ)^2} - \frac{\pi}{10*cos20^\circ} = 0.295521992\ in$$

$$\rho_2 = (r_p + r_g) sin\varphi - \rho_1 = \left(\frac{2.1}{2} + \frac{5.9}{2}\right) * sin20^\circ - 0.295521992 = 1.072558581\ in$$

$$I = \frac{cos\varphi}{\left(\frac{1}{\rho_1} + \frac{1}{\rho_2}\right) d_p} = \frac{cos20^\circ}{\left(\frac{1}{0.296} + \frac{1}{1.073}\right) * 2.1} = 0.103673002$$

Surface stress: $\sigma_c = C_p \sqrt{\frac{W_t}{FId} \frac{C_a C_m}{C_v} C_s C_f} = 1724.498 \sqrt{\frac{327.404*1.6}{1.3*0.104*2.1*0.89}} = 78642.22902\ psi$

Surface-fatigue strength before correction: $S_{fc'} = 349HB + 34300 = 349 * 336 + 34300 = 151564\ psi$

Correction factors of surface-fatigue strength: $C_{L,p} = 2.466 * (N_p)^{-0.056} = 0.833019676$, $C_{L,g} = 2.466 * (N_g)^{-0.056} = 0.873454263$, $C_H = 1$, $C_t = K_t = 0.9097$, $C_r = K_r = 1$

Surface-fatigue strength of pinion: $S_{fc,p} = \frac{C_{L,p} C_H}{C_t C_r} S_{fc'} = \frac{0.833*151564}{0.9097} = 138788.3854\ psi$

Surface-fatigue strength of each gear: $S_{fc,g} = \frac{C_{L,g} C_H}{C_t C_r} S_{fc'} = \frac{0.873*151564}{0.9097} = 145525.1422\ psi$

Surface safety factor of pinion: $N_{c,p} = \frac{S_{fc,p}}{\sigma_c} = \frac{138788.3854}{78642.22902} = 1.76480737$

Surface safety factor of each gear: $N_{c,g} = \frac{S_{fc,g}}{\sigma_c} = \frac{145525.1422}{78642.22902} = 1.850470721$

Summary of correction factors used in gear stress analysis

Table D.10.1 Summary of Correction Factors in Bending Stress

Parameters	Gearset 1	Gearset 2
J_p	0.3404	0.329
J_g	0.4015	0.3885
K_v	0.89	0.92
K_m	1.6	1.6
K_a	1	1
K_s	1	1.25
K_B	1	1
K_I	1	1

Table D.10.2: Summary of Correction Factors in Bending-Fatigue Strength

Parameters	Gearset 1	Gearset 2
$K_{L,p}$	0.900	0.925
$K_{L,g}$	0.925	0.930
K_T	0.9097	0.910
K_R	1	1

Table D.10.3: Summary of Correction Factors in Surface Stress

Parameters	Gearset 1	Gearset 2
C_v	0.89	0.92
C_m	1.6	1.6
C_a	1	1
C_s	1	1.25
I	0.104	0.0974
C_p	1724.50	2300
C_F	1	1
K_R	1	1

Table D.10.4: Summary of Correction Factors in Surface-Fatigue Strength

Parameters	Gearset 1	Gearset 2
$C_{L,p}$	0.833	0.873
$C_{L,g}$	0.873	0.8823
C_T	0.9097	0.910
C_R	1	1
C_H	1	1

Appendix E. Shaft Sample Calculations and Intermediary Results

E.1 FBDs

First, the FBDs for each shaft are constructed and are shown below.

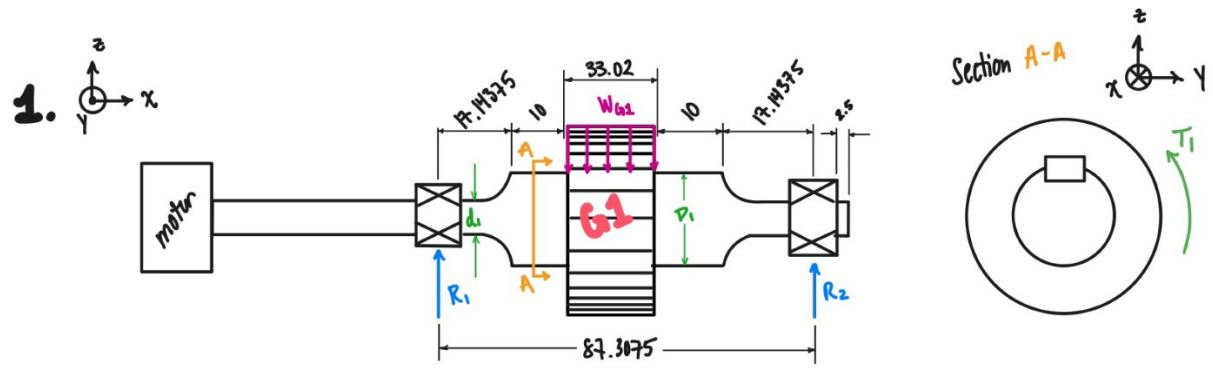

Figure E.1.1: Axial (Left) and Cross-sectional (Right) Free-Body Diagram for the Shaft 2 & 3

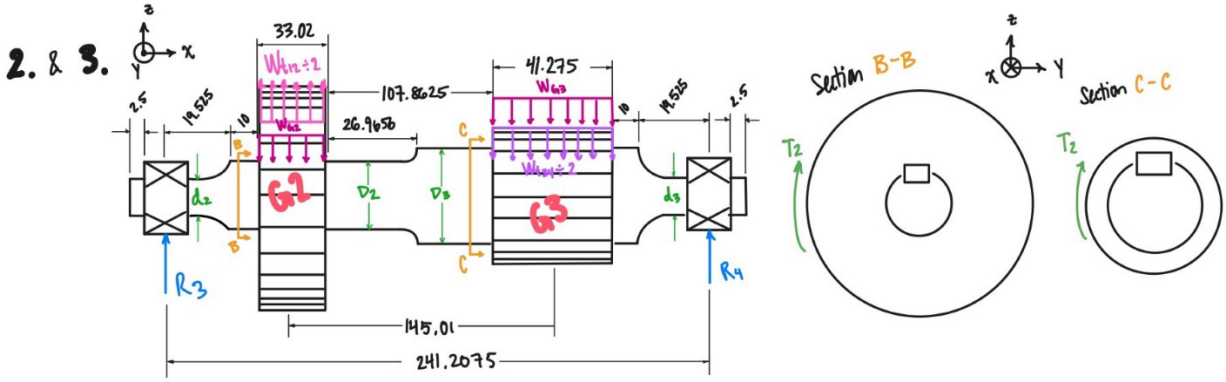

Figure E.1.2: Axial (Left) and Cross-sectional (Right) Free-Body Diagram for the Shaft 2 & 3

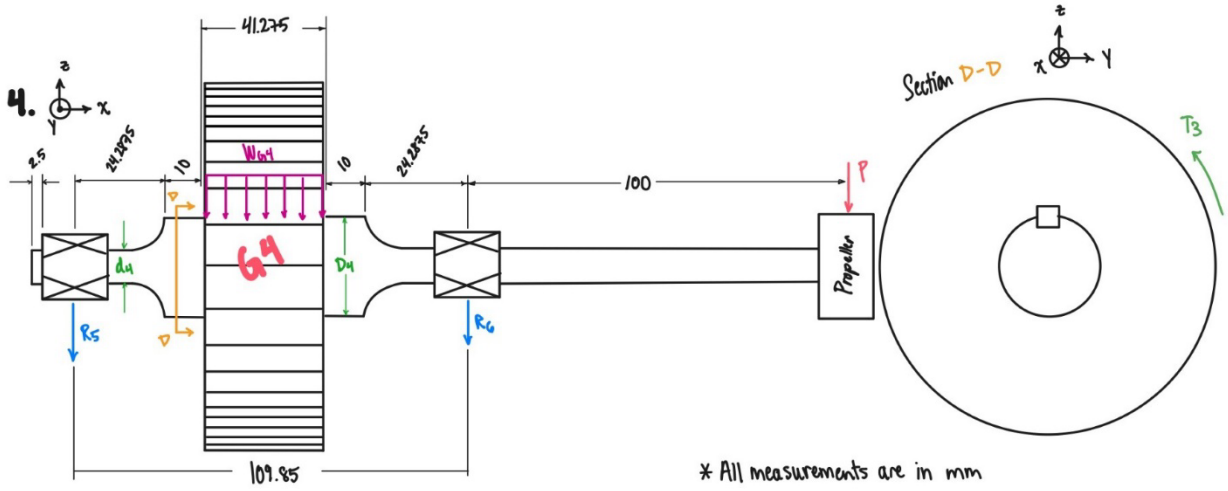

Figure E.1.3: Axial (Left) and Cross-sectional (Right) Free-Body Diagram for the Shaft 4

E.2 Shear and Bending Moment Diagrams

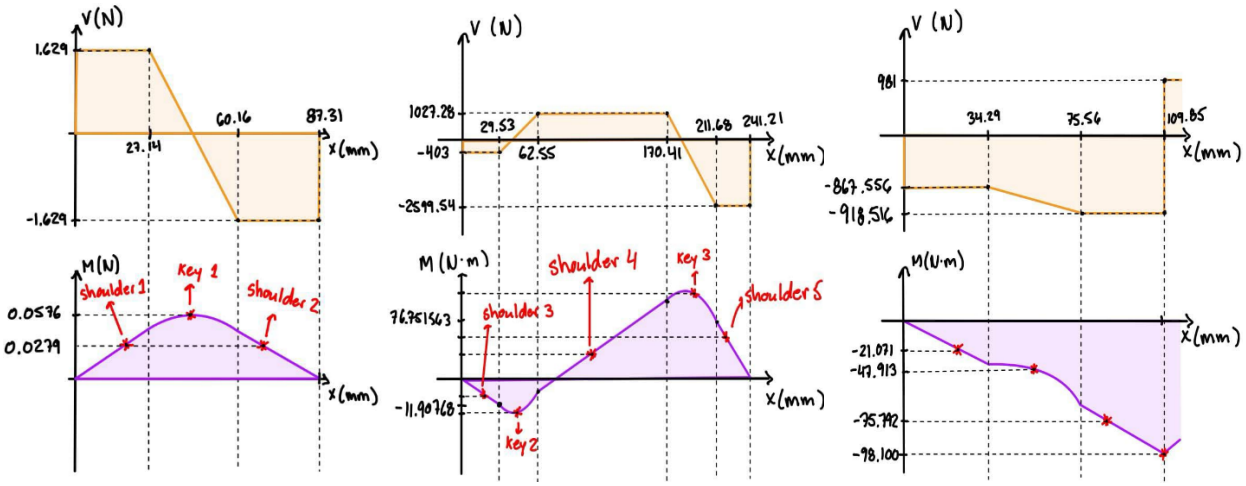

Figure E.2.1: Shear & Bending Moment Diagrams for the Input Shaft (Left), Shaft 2&3 (Middle), and Output Shaft (Right)

Below is provided a sample calculation for the construction of the shear and bending moment diagrams for the input shaft. Note that the same procedure has been followed with the other shafts. First, let us deal with the shear diagram.

We begin by summing the forces in y and the moments about support reaction 1.

$$\sum F_y = -W_{G1} + R_{z,1} + R_{z,2} = -0.332(9.81) + R_{z,1} + R_{z,2} = 0$$

where W_{G1} is the weight of gear 1 acting as a point load at the middle of the gear. Since the mass of gear 1 is already known, its weight is the mass times g. Therefore,

$$\sum F_y = R_{z,1} = -R_{z,2} + 3.257$$

The sum of the moments gives:

$$\sum M_{R1} = -W_{G1}(43.65\ mm) + R_{z,2}(87.31mm)$$

Therefore:

$$R_{z,1} = R_{z,2} = 1.629\ N$$

For the diagrams, the weight from the gear will no longer be considered a point load. Instead, it will be considered as a load distribution along the width of the gear. For the other shafts, the same is true for the tangential forces W_t due to gears. For shaft 1, the load distribution is the weight divided by gear 1' width: $0.09864\ N/mm$. The shear diagram can now be drawn with the load distribution starting at $27.14\ mm$ and ending $60.16\ mm$ as per the FBD. Note that the linear equation describing the load distribution's shear is given by:

$$V = -0.09864x + 4.306$$

The slope of this equation is given by the load distribution's magnitude and orientation, and the variable is computed using the point $(27.14\ mm, 1.629N)$.

For the moment diagram, we must take the integrals of each section of the shear diagram. For the first flat segment, the equation is given by:

$$M_1 = \int 1.629dx = 1.629x \qquad 0 \le x \le 27.14\ mm$$

Using this equation, we can find the bending moment at the first shoulder which is at $17.14\ mm$. The moment at this first critical location is then:

$$M_{shoulder\ 1} = 1.629(17.14)(0.001) = 0.027927\ N \cdot m$$

For the second segment, we take the integral of the function V above:

$$M_2 = \int (-0.09864x + 4.306)dx = -0.04932x^2 + 4.306x + C$$

The integration constant *C* is found using the intersection point between segment 1 and 2, which can be found using $M_1(x)$ above.

$$M_{1-2} = 1.629(27.14)(0.001) = 0.0171\ N \cdot m$$

Plugging this value in $M_2(x)$ gives a value of $C = -36.343$. Hence,

$$M_2 = -0.04932x^2 + 4.306x - 36.343 \qquad 27.14 \leq x \leq 60.16\ mm$$

Thus, the bending moment at the middle point of the shaft, which is at the key, can be found as such:

$$M_{key} = \frac{-0.04932(43.65)^2 + 4.306(43.65) - 36.434}{1000} = 0.0576\ N \cdot m$$

Since the loads are symmetric on shaft 1, only these two points are to be found. For other shafts, they might seem more complicated, but the procedure is the same and does not require further explanation. Once the reaction forces are found, we just have to construct the bending diagrams according to point loads and distributed loads. Then, we take the integrals of the shear equations for each segment and use intersection points to complete the bending moment equations. Next, the critical locations may be analyzed.

E.3 Stress Concentration Factors

For the sample calculation, we will go over the procedure for shaft 4 since it is the most complicated. For the gearbox, stress concentration factors were determined for each iteration of the diameters. Though, for this sample calculation, we will look at the factors for our final design solution.

First, the shoulder fillet with the highest bending moment is analyzed: shoulder 7. For this shoulder, we have a small diameter $d = 0.0295m$ and big diameter $D = 0.0345m$. Also, the fillet radius is $0.005m$. Therefore, we have the following ratios:

$$\frac{D}{d} = 1.16949, \frac{r}{d} = 0.16949$$

Then, the stress concentration factors are computed using *Appendix C.10* to *C.12* for axial load, torsion, and bending. Through, iteration the following coefficients are found:

$$Axial: A = 0.97378, b = -0.23671$$
$$Bending: A = 0.96495, b = -0.22394$$
$$Torsion: A = 0.85342, b = -0.19165$$

Using these coefficients, we find the stress concentration factors:

$$Axial: K_{t,a} = A(\frac{r}{d})^b = 0.97378(0.16949)^{-0.23671} = 1.48$$
$$Bending: K_{t,b} = A(\frac{r}{d})^b = 0.96495(0.16949)^{-0.22394} = 1.44$$
$$Torsion = K_{ts} = A(\frac{r}{d})^b = 0.85342(0.16949)^{-0.19165} = 1.20$$

E.4 Corrected Endurance Limit

The following sample calculation presents the procedure for the corrected endurance limit at the first keyway of shaft 2.

First, we set $C_{load} = 1$ because this shaft is subject to bending and torsion. For size effect, it is assumed that the shaft diameter at the keyway will be between $0.3\ in$ and $10\ in$. Thus, the following equation is used:

$$C_{size} = 0.869d^{-0.097}$$

Obviously, this value was determined once for each iteration of the diameter. Though, for our final iterated diameter, $C_{size} = 0.871$. Shaft 2 being made of cold rolled AISI 1045 steel, we use the following to compute the surface effects:

$$C_{surf} = AS_{ut}^b = 16.841(91000)^{-0.265} = 0.817$$

Note that coefficients A and b are taken from *Appendix B.X*. Also, since the operating temperatures of the gearbox are below $450\ ℃$, and because we assume a 99% reliability, we set:

$$C_{temp} = 1$$
$$C_{reliab} = 0.814$$

The final step is to determine the uncorrected endurance limit of our material. For steels, we have:

$$S_e' = 0.5S_{ut} \qquad \text{for } S_{ut} < 200ksi$$

$$S_e' = 0.5(91000) = 45500\ psi$$

The corrected endurance limit of our shaft is thus:

$$S_e = C_{load}C_{size}C_{surf}C_{temp}C_{reliab}S_e'$$

$$S_e = (1)(0.871)(0.817)(1)(0.814)(45500) = 26342.89\ psi$$

The other endurance limits were computed using a similar approach. The final values are presented in the table below.

Table E.4.1: Corrected Endurance Limits for Each Shaft at Critical Locations

Shaft	Location	$S_e\ [MPa]$
Shaft 1	Shoulder fillet 1	195.38
	Keyway 1	189.01
Shaft 2 & 3	Shoulder fillet 3	187.55
	Keyway 2	181.68
	Shoulder fillet 4	181.68
	Keyway 3	178.82
	Shoulder fillet 5	184.38
Shaft 4	Keyway 4	175.99
	Shoulder fillet 7	178.69
	Bearing 6	179.44

E.5 Shaft Stresses in Shaft 1, 2, and 3

The following sample calculation will present the computation for the maximum stresses occurring in shaft 1 at shoulder fillet 1. Note that the same procedure is used for other critical locations in these shafts.

At this location, the maximum and minimum torque have already been determined and are given by:

$$T_{max} = T_{min} = 77.68\ N \cdot m$$

The alternating and mean components are then found:

$$T_a = \frac{T_{max} - T_{min}}{2} = 0,\ T_m = \frac{T_{max} + T_{min}}{2} = 77.68\ N \cdot m$$

The same procedure is repeated for the alternating and mean components for the bending moments presented in *Table 12*.

$$M_{max} = -M_{min} = 0.02792\ N \cdot m$$

$$M_a = \frac{M_{max} - M_{min}}{2} = 0.02792, \qquad M_m = \frac{M_{max} + M_{min}}{2} = 0\ N \cdot m$$

Then, we have the following stress concentration coefficients whose sample calculation has already been presented.

$$K_t = 0.9305, \qquad K_{ts} = 0.8354$$

Using the *Appendix B.X* ($\sqrt{a}$ table), we have $\sqrt{a} = 0.07$ for $S_{ut} = 91000\ psi$ in bending, and $\sqrt{a} = 0.055$ for $S_{ut} = 91000 + 20000 = 111000\ psi$ in torsion. Then, using the final fillet radius value, $12.7mm = 0.5\ in$, we get the following notch sensitivities:

$$q = \frac{1}{1 + \sqrt{a}/\sqrt{r}}$$

$$Bending: q = 0.9099$$

$$Torsion: q = 0.9278$$

Next, we get the fatigue concentration factors:

$$K_f = 1 + q(K_t - 1) = 1 + 0.9099(0.9305 - 1)$$

$$K_f = 0.9368$$

$$K_{fs} = 1 + q(K_{ts} - 1) = 1 + 0.9278(0.8354 - 1)$$

$$K_{fs} = 0.8472$$

The nominal alternating and mean stress components are found using the final small diameter value:

$$\sigma_{a,nom} = \frac{M_a c}{I} = \frac{32M_a}{\pi d^3} = \frac{32(0.02792)}{\pi(0.011748)^3} = 175398\ Pa = 0.175\ MPa$$

$$\sigma_{m,nom} = \frac{M_m c}{I} = \frac{32M_m}{\pi d^3} = 0$$

$$\tau_{a,nom} = \frac{T_a r}{J} = \frac{16T_a}{\pi d^3} = 0$$

$$\tau_{m,nom} = \frac{T_m r}{J} = \frac{16T_m}{\pi d^3} = \frac{16(77.68)}{\pi(0.011748)^3} = 243998700 = 244.01\ MPa$$

Once this is done, we can get the nominal maximum stresses as such:

$$\sigma_{max,nom} = \sigma_{a,nom} + \sigma_{m,nom} = 0.175MPa$$

$$\tau_{max,nom} = \tau_{a,nom} + \tau_{m,nom} = 244.01MPa$$

Next, we can verify the mean fatigue concentration factors according to the three cases presented in the main body of this report. For torsion, we must use the shear yield strength of the material: $S_{ys} = 0.577S_y = 306.41MPa$.

$$Bending: K_f\sigma_{max,nom} = 0.164\ MPa < S_y = 531.03\ MPa$$

$$Torsion: K_{fs}\tau_{max,nom} = 206.733\ MPa < S_{ys} = 306.41\ MPa$$

Since the first case with no local yielding is observed we have:

$$K_f = K_{fm}$$

$$K_{fs} = K_{fsm}$$

Then, the factors, the alternating and mean torques and moments computed can be used to compute the diameter (see *Appendix E.7)*.

E.6 Shaft Stresses in Shaft 4

The procedure to find the shaft stresses for the last shaft is a bit different than for the others due to the axial load. Hence, the procedure below has been used for various critical locations. This sample calculation will show the procedure used for shoulder fillet 7.

First, let us identify a few important values that will be used whose sample calculation has already been presented.

$M_a = 75.792\ N \cdot m, M_m = 0$

$K_{t,axial} = 1.482, K_{t,bending} = 1.436, K_{ts} = 1.199$

$K_{f,axial} = 1.417, K_{f,bending} = 1.377, K_{fs} = 1.177$

$\sigma_{x,m,bending} = 0, \sigma_{x,a,bending} = 30.072\ MPa, \tau_{a,nom} = 0, \tau_{m,nom} = 102.55\ MPa$

Note that $\sigma_{m,bending}$ and $\sigma_{x,a,bending}$ are the equivalent of $\sigma_{m,nom}$ and $\sigma_{a,nom}$ in the previous sample calculation. For this shaft, we also have to compute a nominal alternating and mean stress component for the axial load as follows:

$$\sigma_{x,axial,max} = \frac{F}{A} = \frac{4(4448)}{\pi(0.0295)^2} = 6507750\ Pa = 6.508\ MPa = \sigma_{x,axial,min}$$

Note that *F* is the axial load, and that the max and min stress from this load are equal since the load is constant. Using the same formula for mean and alternating components, we have:

$$\sigma_{x,m,axial} = 6.508\ MPa, \sigma_{x,a,axial} = 0$$

Then, we must find the nominal combined multiaxial alternating and mean stresses:

$$\sigma_{a,nom} = \sqrt{{\sigma_{x,a,bending}}^2 + 3{\tau_{a,nom}}^2} = 30.072\ MPa$$

$$\sigma_{m,nom} = \sqrt{(\sigma_{x,m,bending} + \sigma_{x,m,axial})^2 + 3{\tau_{m,nom}}^2} = 177.734\ MPa$$

Using these, we find:

$$\sigma_{max,nom} = \sigma_{a,nom} + \sigma_{m,nom} = 207.806\ MPa$$

Like the other shafts, we must verify for the mean fatigue concentration factor for axial load, bending, and torsion.

$$K_{f,axial}\sigma_{max,nom} = 294.367\ MPa < S_y = 531.03\ MPa$$
$$K_{f,bending}\sigma_{max,nom} = 286.048\ MPa < S_y = 531.03\ MPa$$
$$K_{fs}\tau_{max,nom} = 120.721\ MPa < S_{ys} = 306.31\ MPa$$

Therefore,

$$K_{f,axial} = K_{fm,axial}, K_{f,bending} = K_{fm,bending}, K_{fs} = K_{fsm}$$

Finally, before iterating for a safety factor, we must find the maximum combined stresses (those that includes the fatigue factors).

$$\sigma'_a = \sqrt{\left(K_{f,bending}\sigma_{x,a,bending}\right)^2 + 3\left(K_{fs}\tau_{a,nom}\right)^2} = 41.394\ MPa$$

$$\sigma'_m = \sqrt{(K_{fm,bending}\sigma_{x,m,bending} + K_{fm,axial}\sigma_{x,m,axial})^2 + 3(K_{fsm}\tau_{m,nom})^2} = 209.298\ MPa$$

The safety factor can now be computed (see *Appendix E.8* below).

E.7 Diameters for Shaft 1,2 & 3

The following sample calculation will show the process of calculating the small diameter of shaft 1. Note that the same formula and approach as been used for the other diameters.

First, let us highlight various values that will be used:

$M_a = 0.027918\ N\cdot m, \quad M_m = 0\ N\cdot m, \quad T_a = 0\ N\cdot m, \quad T_m = 77.68\ N\cdot m$
$K_f = 0.9367 = K_{fm}, \quad K_{fs} = 0.8472 = K_{fsm}$
$N_f = 1.75$
$S_e = 195.38\ MPa, \quad S_{ut} = 627.59\ MPa$

Then, we use equation (xx):

$$d = \left\{\frac{32N_f}{\pi}\left[\frac{\sqrt{(K_f M_a)^2 + 0.75(K_{fs}T_a)^2}}{S_e} + \frac{\sqrt{(K_{fm}M_m)^2 + 0.75(K_{fsm}T_m)^2}}{S_{ut}}\right]\right\}^{1/3}$$

$$d = \left\{\frac{32(1.75)}{\pi}\left[\frac{\sqrt{(0.9367\cdot 0.02792)^2 + 0.75(0)^2}}{195.38} + \frac{\sqrt{(0)^2 + 0.75(0.8472\cdot 77.68)^2}}{627.59}\right]\right\}^{1/3}$$

$$d = 11.75\ mm$$

E.8 Safety Factors for Shaft 4

As mentioned, for the output shaft, the procedure differs in the sense that we iterated for a safety factor due to the complexity of isolating for a diameter. The subsequent sample calculation is that of the safety factor at shoulder fillet 7. To test the safety factor of a given diameter, we first compute the mean and alternating combined multiaxial stresses as shown above. At this location, these stresses are:

$$\sigma'_a = 41.394\ MPa$$
$$\sigma'_m = 209.298\ MPa$$

We also have the corrected fatigue strength at this location: $S_e = 178.69\ MPa$. Finally, the safety factor is found using equation (x):

$$\frac{1}{N_f} = \frac{\sigma'_a}{S_e} + \frac{\sigma'_m}{S_{ut}}$$

$$N_f = \left[\frac{41.394}{178.69} + \frac{209.298}{627.59}\right]^{-1} = 1.77$$

This process has been done a number of times with various diameters in order to get a value close to and greater than 1.75.

E.9 Yielding Factor of Safety

To compute the yielding factor of safety, one must first obtain the combined multiaxial stresses in the shaft at the location of interest. In this case, we will look at shoulder fillet 3 in shaft 2.

$$\sigma_a = \sqrt{(K_t\sigma_{a,bending})^2 + 3(K_{ts}\tau_a)^2}$$

$$\sigma_a = \sqrt{(1.033 \cdot 13.96)^2 + 3(0.9209 \cdot 0)^2} = 14.426\ MPa$$

$$\sigma_m = \sqrt{(K_t\sigma_{m,bending})^2 + 3(K_{ts}\tau_m)^2}$$

$$\sigma_m = \sqrt{(1.033 \cdot 0)^2 + 3(0.9208 \cdot 193.48)^2} = 310.517\ MPa$$

Note that the shaft stresses and stress concentration factors have been computed using the procedures already presented above. We then find the yielding safety factor using equation (40) and (41) as such:

$$N_y = \frac{S_y}{\sigma_{max}} = \frac{531.03}{14.426 + 310.517} = 1.63$$

The other yielding safety factors computed using this approach are presented in *Table E.9.1* below.

Table E.9.1: Yielding Safety Factors for Static Failure During the First Cycle at Various Locations

Shaft	Location	Yielding Safety Factor N_y
Shaft 1	Shoulder Fillet 1	1.48
	Keyway 1	1.48
Shaft 2 & 3	Shoulder Fillet 3	1.63
	Keyway 2	1.64
	Shoulder Fillet 4	2.87
	Keyway 3	1.92
	Shoulder Fillet 5	2.21
Shaft 4	Keyway 4	2.07
	Shoulder Fillet 7	1.48
	Bearing 6	2.15

Appendix F. Key Sample Calculations and Intermediary Results

F.1 Shear Fatigue

The key geometry is determined by the corresponding shaft diameter. At location 1, the diameter of the shaft is shown in the *Table F.1.1* below.

Table F.1.1: Key Geometries of the First Key at Keyway 1

Diameter of the shaft	Key width	Key height	Key length
16.53 mm	5 mm	5 mm	33.02 mm (Gear face width)

The Von Mises stress can be calculated from the equation (46) and (47) shown in section *3.3.3*:

$$\sigma_a{}' = \sqrt{\sigma_{x,a}^2 + \sigma_{y,a}^2 - \sigma_{x,a}\sigma_{y,a} + 3\tau_{xy,a}^2} = \sqrt{0.13^2} = 0.13\ MPa$$

$$\sigma_m{}' = \sqrt{\sigma_{x,m}^2 + \sigma_{y,m}^2 - \sigma_{x,m}\sigma_{y,m} + 3\tau_{xy,m}^2} = \sqrt{3 \times 87.55^2} = 151.64\ MPa$$

Given the ultimate tensile strength of the material is smaller than 1400 MPa, the uncorrected endurance limit of the material is given as:

$$Se' = 0.5S_{ut} = 0.5 \times 469\ MPa = 234.5\ MPa$$

Since the function of the key is to transmit torque and power, bending stress and torsion stress can occur. Thus, the loading correction factor is determined to be: $C_{load} = 1$.

The geometric correction factor is determined using an equivalent area A_{95}.

$$A_{95} = 0.05 \times 5^2 = 1.25\ mm^2$$

$$d_{eq} = \sqrt{\frac{1.25}{0.0766}} = 4.03\ mm$$

The equivalent diameter of the key is smaller than 5 mm. Thus, the size correction factor is determined to be: $C_{size} = 1$.

The surface finish correction factor is determined using the following equations:

$$A = 4.51 \qquad b = -0.265 \qquad C_{surf} = 4.51{S_{ut}}^{-0.265}$$

$$C_{surf} = 4.51(469)^{-0.265} = 0.884$$

The working temperature of the key is not within the high temperature range. Therefore, the temperature correction factor is: $C_{temp} = 1$.

Given the common 99% reliability in the aerospace industry, the reliability correction factor is determined as: $C_{reliab} = 0.814$. *Table F.1.2* below summarizes the correction factors for the keys used in this gearbox design.

Table F.1.2: Correction Factors for Different Keys

Correction Factors	Key 1	Key 2 and 2'	Key 3 and 3'	Key 4
C_{load}	1	1	1	1
C_{surf}	0.88257783	0.88257783	0.88257783	0.88257783
C_{size}	1	1	1	1
C_{temp}	1	1	1	1
C_{reliab}	0.814	0.814	0.814	0.814

Now, the corrected endurance limit can be calculated.

$$Se = 0.884 \times 0.814 \times 234.5 = 168.688\ MPa$$

The fatigue factor of safety can be determined from the Case 3 scenario:

$$N_{fs} = \frac{1}{\frac{\sigma_a{}'}{Se} + \frac{\sigma_m{}'}{S_{ut}}} = 3.09$$

F.2 Bearing Failure

The bearing failure safety factor is determined by treating it as a static failure scenario. The bearing area of a typical square key is:

$$A_{bearing} = \frac{Lh}{2} = 33.02 \times 5 \times 0.5 = 82.55\ mm^2$$

The bearing force can be calculated from the maximum torque transmitted by the shaft and the radius of the shaft.

$$F_{max} = \frac{T_{max}}{16.53/2} = \frac{77.68 \times 10^3}{16.53/2} = 9398.669\ N$$

$$\sigma_{max} = \frac{F_{max}}{A_{bearing}} = \frac{9398.669\ N}{82.55\ mm^2} = 113.854\ MPa$$

Then, the bearing failure safety factor can be determined as the following:

$$N_{fs} = \frac{S_y}{\sigma_{max}} = \frac{393\ MPa}{113.854\ Mpa} = 3.45$$

Appendix G. Bearing Sample Calculation and Intermediary Results

G.1 Bearing Required Life

The following sample calculation presents how the required life for bearing 3 and 4 was computed. Note that the same procedure was repeated for the other bearings, only changing the angular velocity according to the shaft.

$$L = \omega \Delta t$$

where Δt is the desired life of the gearbox: 2000 hours. The angular velocity of the second shaft, and by the same, that of the bearings, is: $1957.63\ RPM$ as previously computed.

$$L = (1957.63)(60)(2000)$$
$$L = 234.915\ millions\ of\ revolutions$$

G.2 L_{10} Life and Bearing Parameters

The sample calculation below presents the procedure used for bearing 6. This bearing is the most complicated since accounting for the axial loads is required. First, we select a bearing that matches our shaft diameter: $30\ mm$. In this case, we selected the 32006 X bearing from the SKF catalogue which has the following parameters:

$$C_0 = 44000\ N, \qquad C = 43900\ N,$$

Then, the radial and axial forces must be computed. The axial load is $1000\ lbf = 4448\ N$ and is given. The radial force is simply the reaction force at this bearing location: $1899.52\ N$, and was determined during the shaft analysis when the shear and bending moment diagrams were made. The following ratio is computed:

$$\frac{F_a}{C_0} = \frac{4448}{44000} = 0.1011$$

Figure C.18 is then used to find a factor *e* by interpolation. We get the following value:

$$e = 0.2931$$

Then, we verify the following for single row bearings:

$$\frac{F_a}{VF_r} > e$$
$$\frac{4448}{(1)(1899.52)} > 0.2931$$

Here, the value of *V* is set at 1 because the inner ring is rotating with respect to the load. This is true for the other bearings of the gearbox as well. Using the corresponding column in *Figure C.18*, we get the following factor:

$$X = 0.56 \qquad Y = 1.484$$

And the equivalent load *P* is computed:

$$P = XVF_r + YF_a$$
$$P = 0.56(1)(1899.52) + 1.484(4448) = 7665.74$$

Note that for the other bearings where the axial load was not present, the equivalent load *P* was directly taken as the radial force at the bearing location, i.e. the reaction force from the shaft analysis. Then, the L_{10} life is computed.

$$L_{10} = \left(\frac{C}{P}\right)^{10/3} = \left(\frac{43900}{7665.74}\right)^{10/3} = 336.022\ millions\ of\ revolutions$$

This is higher than the required life, therefore the bearing is appropriate. Note that the following equation was used for the other bearings since they are ball bearings rather than roller bearings:

$$L_{10} = \left(\frac{C}{P}\right)^{3}$$

The table below presents key parameters of the selected bearings that were used during computations:

Table G.2.1: Key Parameters of the Selected Bearings

Bearing location	Designation from SKF	Dynamic Load Rating C [N]	Static Load Rating C_0 [N]
Bearing 1 & 2	6001	5400	2360
Bearing 3 & 4	63/22	18600	9300
Bearing 5	16006	11900	7350
Bearing 6	32006 X	43900	44000

G.3 SKF Bearing Catalogue Screenshots

Designation	Principal dimensions			Basic load ratings		Speed ratings	
				dynamic	static	Reference speed	Limiting speed
	d [mm]	D [mm]	B [mm]	C [kN]	C_0 [kN]	[r/min]	[r/min]
W 63800 R-2Z	10	19	7	1.48	0.83	80 000	38 000
W 63800-2Z	10	19	7	1.48	0.83	80 000	38 000
16101	12	30	8	5.07	2.36	60 000	38 000
16101-2RS1	12	30	8	5.07	2.36		17 000
16101-2Z	12	30	8	5.07	2.36	56 000	28 000
4201 ATN9	12	32	14	10.6	6.2	36 000	20 000
4301 ATN9	12	37	17	13	7.8	34 000	18 000
6001	12	28	8	5.4	2.36	60 000	38 000
6001-2RSH	12	28	8	5.4	2.36		17 000

Figure G.3.1: SKF Catalogue for Deep Groove Ball Bearings 1 & 2

Designation	Principal dimensions			Basic load ratings		Speed ratings	
				dynamic	static	Reference speed	Limiting speed
	d [mm]	D [mm]	B [mm]	C [kN]	C_0 [kN]	[r/min]	[r/min]
W 6304	20	52	15	13.8	7.8	34 000	20 000
W 6304-2RS1	20	52	15	13.8	7.8		9 500
W 6304-2Z	20	52	15	13.8	7.8	34 000	17 000
62/22	22	50	14	14	7.65	30 000	19 000
62/22-2RS1	22	50	14	14	7.65		9 000
63/22	22	56	16	18.6	9.3	28 000	18 000
16005	25	47	8	8.06	4.75	32 000	20 000

Figure G.3.2: SKF Catalogue Picture for Deep Groove Ball Bearings 3 & 4

Designation	Principal dimensions			Basic load ratings		Speed ratings	
				dynamic	static	Reference speed	Limiting speed
	d [mm]	D [mm]	B [mm]	C [kN]	C_0 [kN]	[r/min]	[r/min]
W 6205-2RS1	25	52	15	11.7	7.65		8 500
W 6205-2RS1/VP311	25	52	15	11.7	7.65		8 500
W 6205-2Z	25	52	15	11.7	7.65	30 000	15 000
W 6305	25	62	17	17.8	11.2	26 000	17 000
W 6305-2RS1	25	62	17	17.8	11.2		7 500
W 6305-2Z	25	62	17	17.8	11.2	26 000	13 000
62/28	28	58	16	16.8	9.5	26 000	16 000
16006	30	55	9	11.9	7.35	28 000	17 000
206	30	62	16	20.9	16.3	20 000	12 000

Figure G.3.3: SKF Catalogue Picture for Deep Groove Ball Bearing 5

Designation	Principal dimensions			Basic load ratings		Speed ratings	
				dynamic	static	Reference speed	Limiting speed
	d [mm]	D [mm]	T [mm]	C [kN]	C_0 [kN]	[r/min]	[r/min]
322/28 B	28	58	20.25	51.9	50	9 500	12 000
1988/1922	28.575	57.15	19.845	58.2	55	10 000	12 000
30206	30	62	17.25	50	44	9 000	11 000
30306	30	72	20.75	69.2	56	8 000	10 000
31306	30	72	20.75	58.3	50	7 500	9 500
32006 X	30	55	17	43.9	44	10 000	12 000

Figure G.3.4: SKF Catalogue Screenshot for Tapered Roller Bearing 6

Appendix H. Assembly Models, Exploded Views, Drawings, and Other Pictures

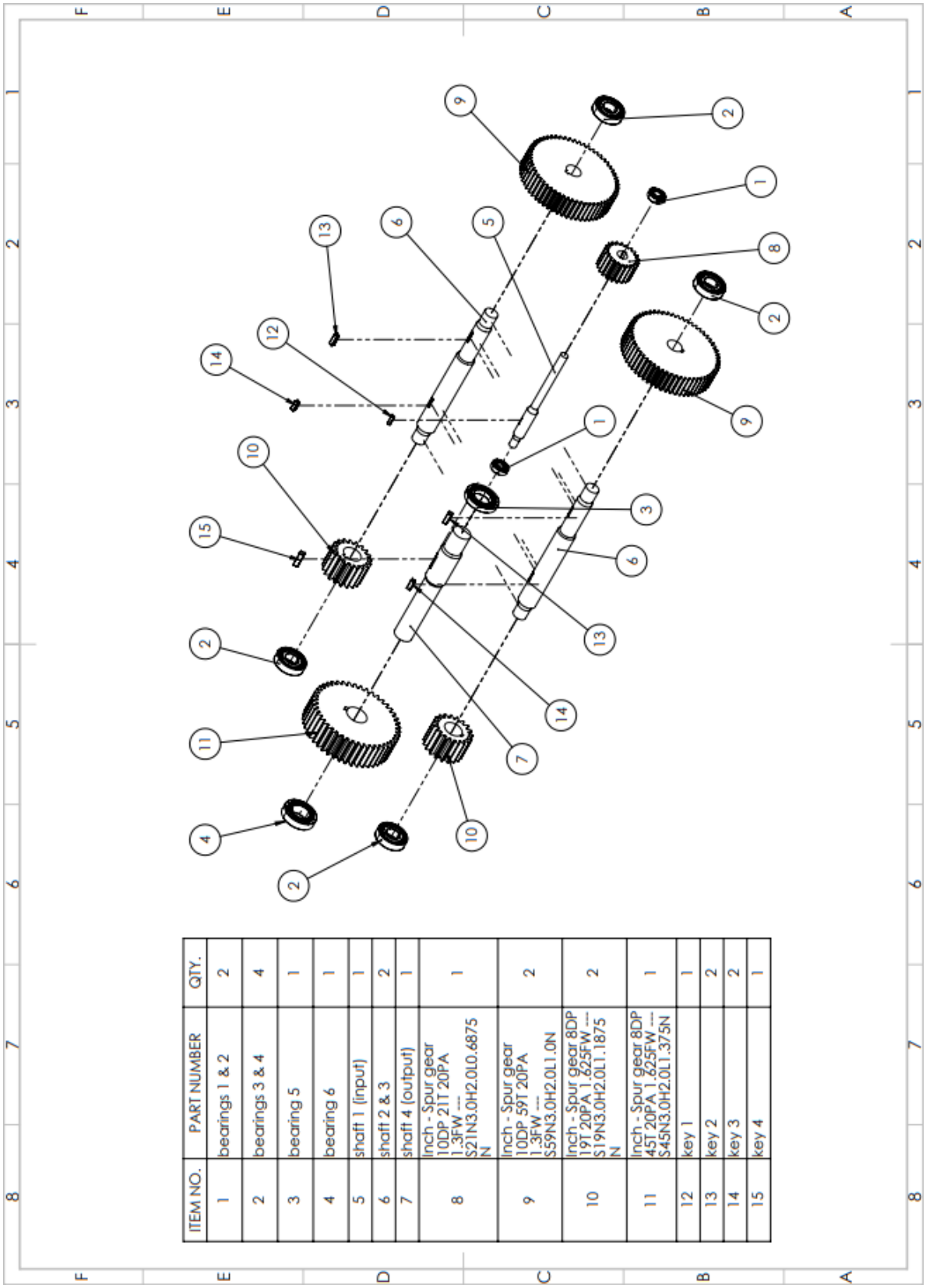

ITEM NO.	PART NUMBER	QTY.
1	bearings 1 & 2	2
2	bearings 3 & 4	4
3	bearing 5	1
4	bearing 6	1
5	shaft 1 (input)	1
6	shaft 2 & 3	2
7	shaft 4 (output)	1
8	Inch - Spur gear 10DP 21T 20PA 1.3FW --- S21N3.0H2.0L0.6875 N	1
9	Inch - Spur gear 10DP 59T 20PA 1.3FW --- S59N3.0H2.0L1.0N	2
10	Inch - Spur gear 8DP 19T 20PA 1.625FW --- S19N3.0H2.0L1.1875 N	2
11	Inch - Spur gear 8DP 45T 20PA 1.625FW --- S45N3.0H2.0L1.375N	1
12	key 1	1
13	key 2	2
14	key 3	2
15	key 4	1

Figure H.1: Exploded View of the Gearbox Assembly

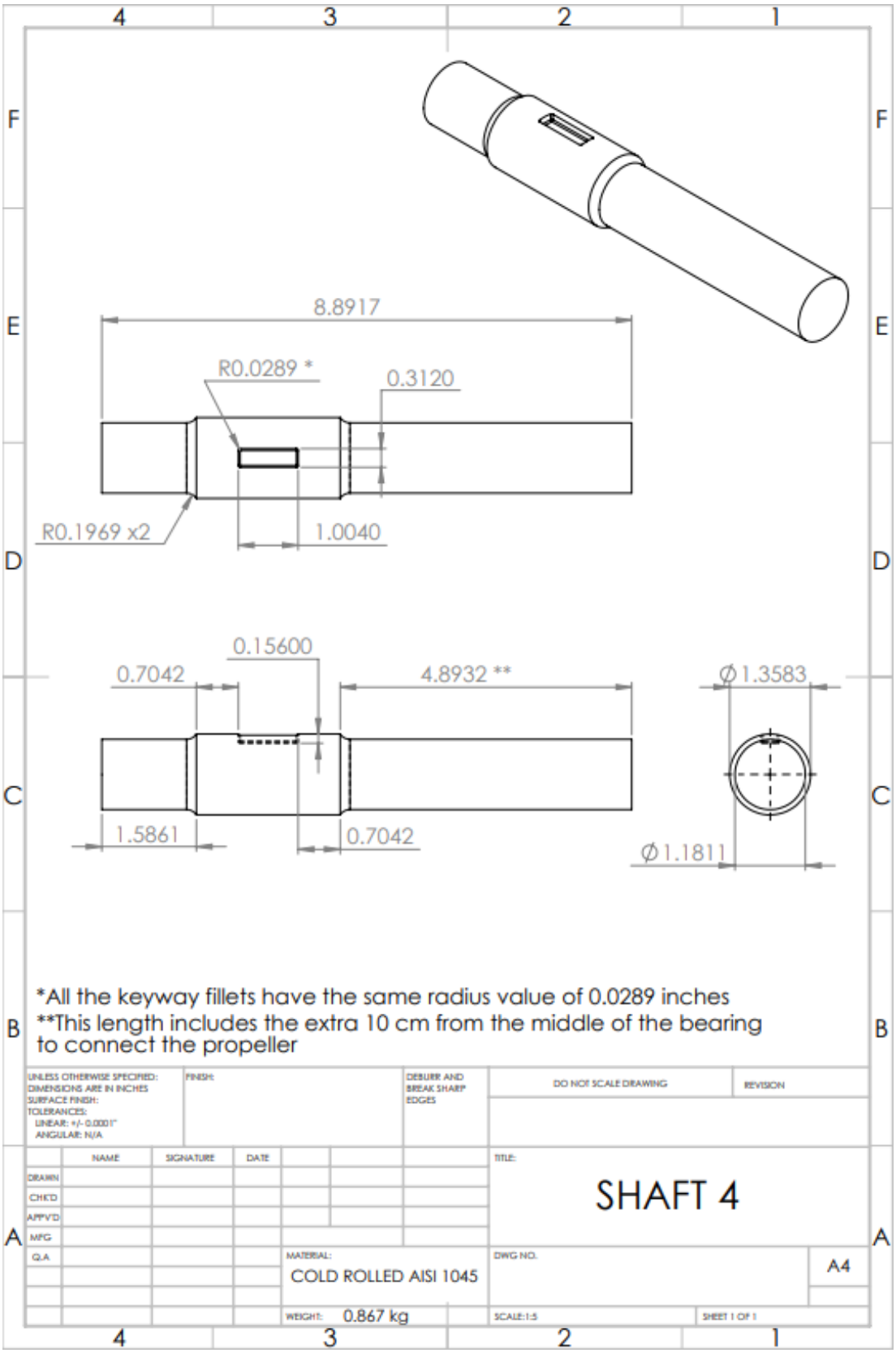

Figure H.2: Engineering Drawing of Output Shaft 4

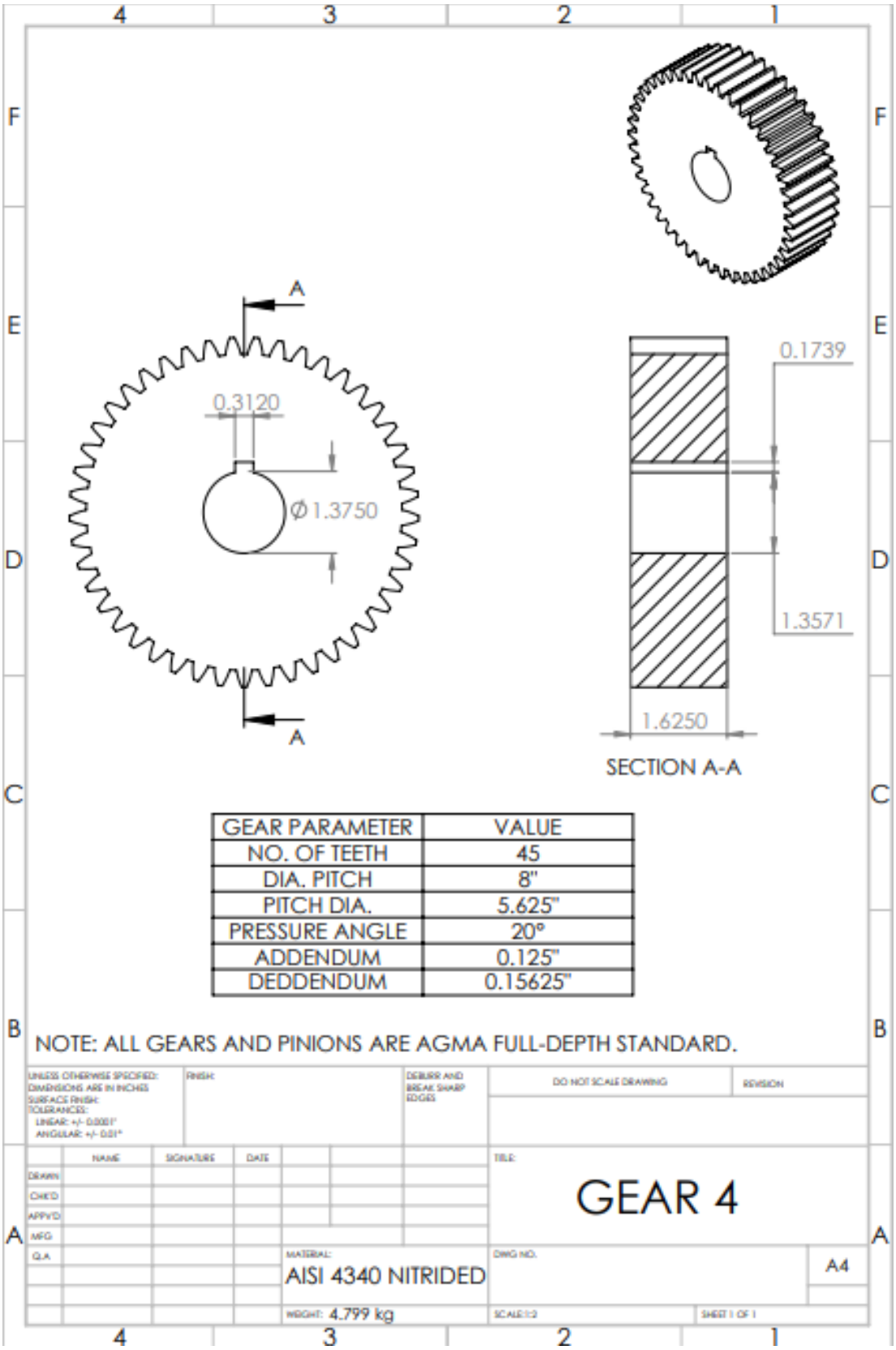

Figure H.3: Engineering Drawing of Gear 4

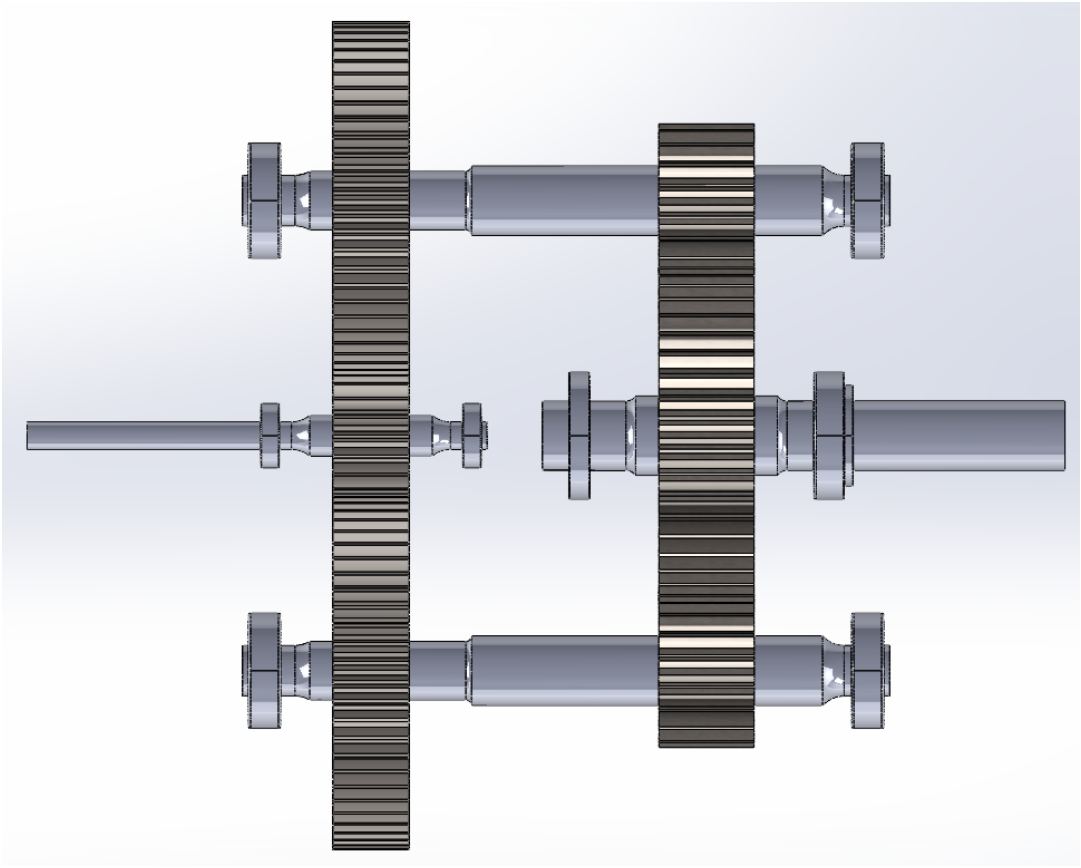

Figure H.4: Top view of the Gearbox Assembly

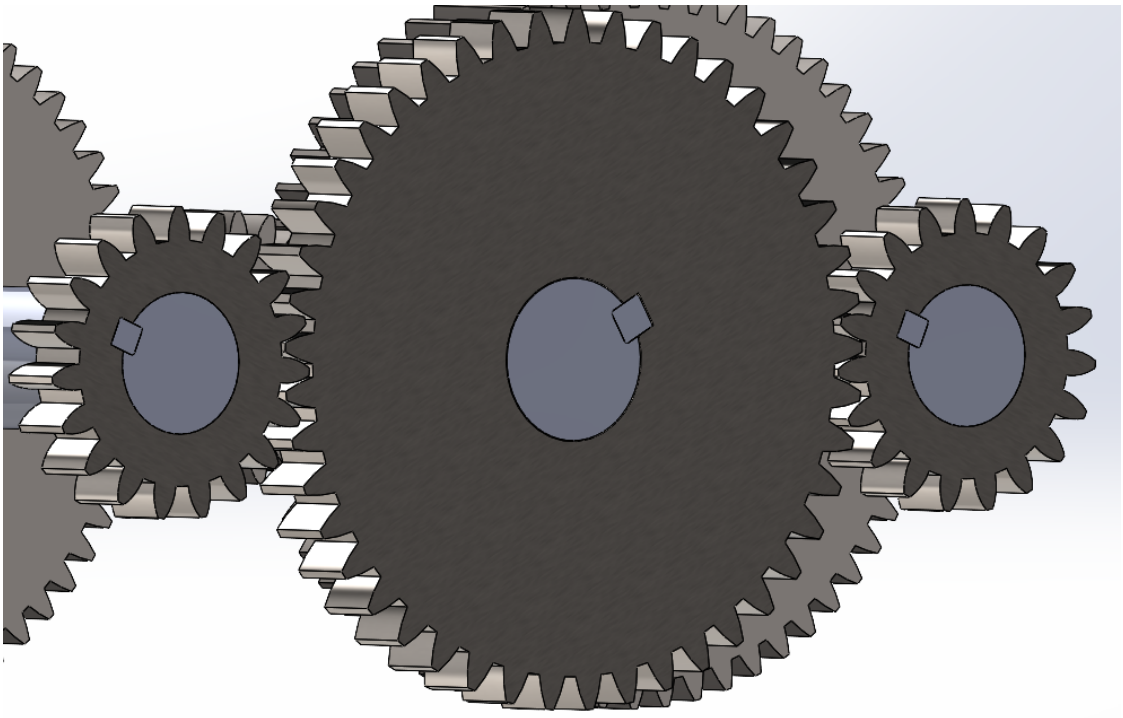

Figure H.5: Section View of Gears 3, 3', and 4 with their Respective Key in Place